Online Coupling of Liquid Chromatography to Raman Spectroscopic Detection for the Analysis of Proteins and Other Biopharmaceutical Products

Inaugural-Dissertation

zur Erlangung des Doktorgrades
der Mathematisch-Naturwissenschaftlichen Fakultät
der Heinrich-Heine-Universität Düsseldorf

vorgelegt von

Jana Thißen
aus Geldern

Düsseldorf, Februar 2026

aus dem Institut für Pharmazeutische Technologie und Biopharmazie
der Heinrich-Heine-Universität Düsseldorf

Gedruckt mit der Genehmigung der
Mathematisch-Naturwissenschaftlichen Fakultät der
Heinrich-Heine-Universität Düsseldorf

Berichterstatter:

1. Prof. Dr. Jörg Breitkreutz

2. Jun.-Prof. Dr. Michael C. Hacker

Tag der mündlichen Prüfung: 19. August 2026

Für meine Familie

Table of Content

List of Abbreviations

AC	affinity chromatography
ADCC	antibody-dependent cellular cytotoxicity
ALS	asymmetric least-squares
bLG	β-lactoglobulin
BSA	bovine serum albumin
BVCZ	bevacizumab
c	speed of light
CCD	charge coupled device
CERS	capillary-enhance Raman spectroscopy
CHO	Chinese hamster ovary
D	number density of scatterers
DAD	diode-array detector
DRTM	daratumumab
dz	pathlength of the laser in a sample
E	energy
E_0	electronic ground state
E_1	first excited electronic state
EC50	half-maximal effective concentration
E_F	electric field of a photon
ELSD	evaporative light scattering detection
F_{ab}	fragment antigen binding sites
FAIR	findable, accessible, interoperable and reusable
F_c	fragment crystallizable
FDA	U.S. Food and Drug Administration
h	Planck’s constant
Hb	hemoglobin
HEWL	hen egg white lysozyme
HIC	hydrophobic interaction chromatography
HILIC	hydrophilic interaction chromatography

HPLC	high-performance liquid chromatography
HQI	hit quality index
IEX	ion-exchange chromatography
IgG	immunoglobulin G
I_R	intensity of Raman scattering
I_0	laser intensity
LC	liquid chromatography
LCW	liquid core waveguide
LOD	limit of detection
LOQ	limit of quantification
MCR-ALS	multivariate curve resolution alternating least squares
MS	mass spectrometry
N_0	vibrational ground state
N_1	first excited vibrational state
P	polarization
PBS	phosphate buffered saline
PCA	principal component analysis
PSA	porcine serum albumin
PTMs	post-translational modifications
Q_j	oscillation of a normal mode
RI	refractive index detection
RP	reversed-phase chromatography
RRS	resonance Raman spectroscopy
RS	Raman spectroscopy
RTX	rituximab
SEC	size exclusion chromatography
SERS	surface-enhanced Raman spectroscopy
SNR	signal-to-noise ratio
SSC	stainless-steel capillary
t	time
VFT	vertical flow technique

VN_1	virtual level 1
VN_2	virtual level 2
α	polarizability
λ	wavelength
μ'	optical constant
v	frequency
σ_j	Raman scattering cross section
$\tilde{\nu}$	wavenumber

1 Introduction

1.1 Raman spectroscopic detection for liquid chromatography

The main goal of the present thesis is to couple Raman spectroscopic detection with liquid chromatography (LC) for the analysis of proteins. Therefore, Chapter 1.1 provides an overview of the theoretical background of Raman scattering and summarizes the current state of research on Raman spectroscopic detection for LC.

1.1.1 Classical description of Raman scattering

If monochromatic light encounters a molecule, there is a chance that the light interacts with the molecule. For example, the light can be scattered either elastically or inelastically. In general, light can be described by equation (1).

$$E = h \cdot v = \frac{h \cdot c}{\lambda} \tag{1}$$

with E = Energy, h = Planck's constant, v = frequency, c = speed of light, λ = wavelength

Given by equation (1), the energy of a photon is proportional to its frequency and reciprocal to its wavelength. The wavenumber is defined by equation (2).

$$\tilde{\nu} = \frac{v}{c} = \frac{1}{\lambda} \tag{2}$$

with $\tilde{\nu}$ = wavenumber, v = frequency, c = speed of light, λ = wavelength

Owing to historical convention, the Raman shift of various modes is commonly expressed in wavenumbers instead of frequencies or wavelengths. The content of this chapter, which outlines the classical description of Raman scattering and some intensity considerations, is based on McCreery's book[1, 2].

The oscillating electric field of the incident photon induces polarization in the molecule. This leads to an induced dipole in the molecule that radiates scattered light either with (inelastic scattering) or without exchanging energy (elastic scattering). The polarization of the molecule *P* is dependent on its polarizability *α* and the oscillating electric field of the incident photon E_F as shown in equation (3).

$$P = \alpha \cdot E_F \tag{3}$$

The electric field of the incident photon E_F can be described according to equation (4).

$$E_F = E_0 \cdot \cos 2\pi\nu_0 t \tag{4}$$

The electric field of the incident photon oscillates at its frequency ν_0. In a non-linear molecule with N atoms, there are $3N-6$ normal modes Q_j which combine to form molecular vibrations. Equation (5) describes the oscillation of a normal mode Q_j at the characteristic harmonic frequency ν_j of the j^{th} normal mode.

$$Q_j = Q_j^0 \cdot \cos 2\pi\nu_j t \tag{5}$$

The polarizability of a molecule α can be influenced by molecular vibrations according to the classical treatment of Raman scattering. This is given by equation (6).

$$\alpha = \alpha_0 + \left(\frac{\delta\alpha}{\delta Q_j}\right) Q_j + \cdots \tag{6}$$

If equations (4) and (6) are substituted into equation (3), equation (7) describing the polarization P is obtained by applying the trigonometric product-sum identities and neglecting higher terms.

$$P = \alpha_0 E_0 \cos 2\pi\nu_0 t + E_0 Q_j^0 \left(\frac{\delta\alpha}{\delta Q_j}\right) \frac{\cos 2\pi(\nu_0 + \nu_j)\, t + \cos 2\pi(\nu_0 - \nu_j)\, t}{2} \tag{7}$$

According to equation (7) light will be scattered at three frequencies, assuming the polarized electrons will emit light at the frequency of their oscillations. The first term is elastic scattering, i.e. Rayleigh scattering, whereas the second and third terms are inelastic scattering, i.e. Raman scattering. In Rayleigh scattering, the light is scattered at the same frequency as the laser, with the magnitude of scattered light being proportional to the inherent polarizability α_0 of the molecule. Anti-Stokes scattering is described by $\nu_0 + \nu_j$ while Stokes scattering is described by $\nu_0 - \nu_j$. From equation (7) can be taken that Raman scattering can only occur if vibrational modes lead to a change in polarizability $\delta\alpha/\delta Q \neq 0$. This is the selection rule for Raman scattering.

Figure 1-1 provides an overview of the scattering processes that can occur. In Rayleigh scattering, the incident light $h\nu_0$ is scattered elastically meaning that the incoming and the scattered light have the same frequency ν_0. The molecule gets excited to a virtual

state VN_1 within the scattering process which can be considered as a very short-lived distortion of the electron cloud induced by the electric field of the laser light.

Stokes and Anti-Stokes Raman scattering can be distinguished depending on the energy of the scattered light. A molecule in its vibrational ground state N_0 gets excited by a laser photon hv_0 and thus reaches a virtual state VN_1. Then, the light is scattered from the molecule, leaving the molecule in an excited vibrational state N_1 due to absorption of a certain amount of energy v_j. The scattered light has therefore a lower frequency than the incident light beam $(v_0 - v_j) < v_0$ which is referred to as Stokes scattering. In Anti-Stokes scattering, the molecule is in the first excited vibrational state N_1 when it gets excited by a laser photon hv_0. Then, a certain amount of energy is transferred with the scattered light v_j resulting in a higher frequency of the scattered light $(v_0 + v_j)$ in comparison to the incident light $(v_0 + v_j) > v_0$ and leaving the molecule in its vibrational and electronic ground state N_0, E_0 after the interaction. Both processes are Raman scattering processes.

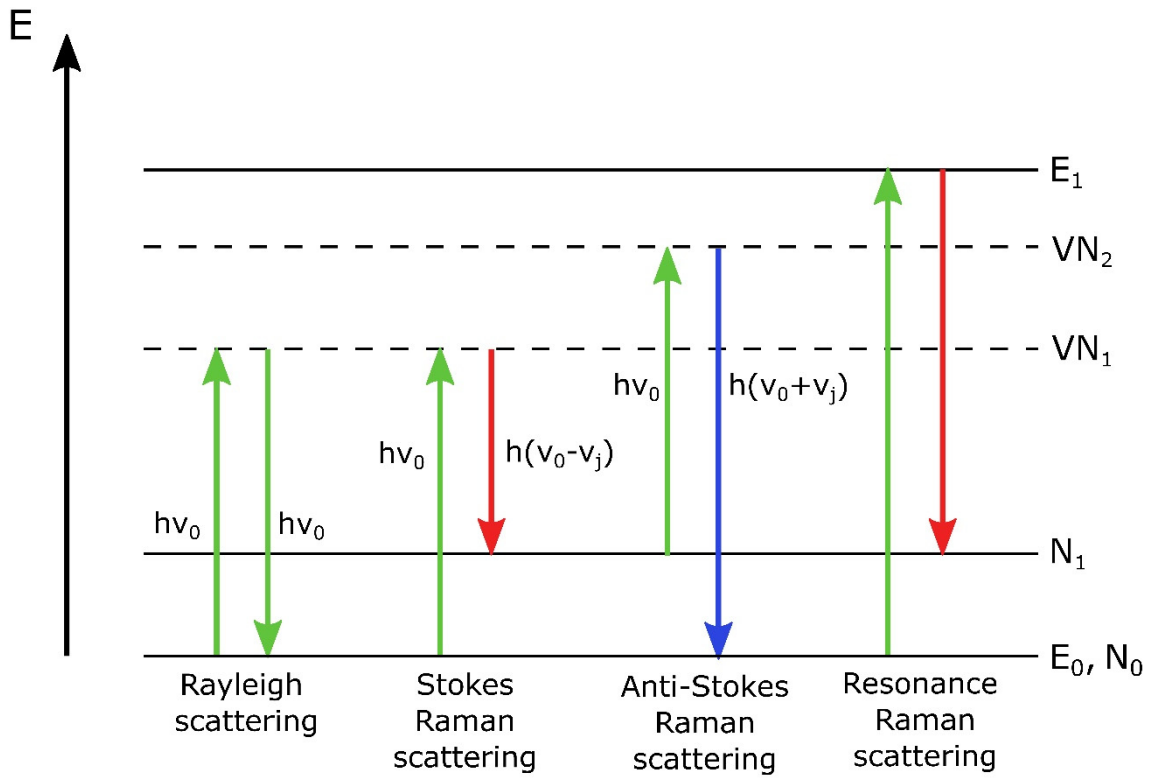

Figure 1-1: Energy level scheme to describe the different elastic and inelastic scattering processes.

The observed intensity of Raman scattering I_R can be described by equation (8).

$$I_R = \mu' \left(\bar{\nu}_0 \pm \bar{\nu}_j\right)^4 \alpha_j^2 Q_j^2 \qquad (8)$$

where μ' is a constant containing the factor c^4 as the intensity is expressed in wavenumbers instead of frequency following the relation shown in equation (2). Equation (8) indicates that the Raman intensity is proportional to the fourth power of the observed wavenumber, which on the other hand depends on the laser frequency. Therefore, the intensity varies proportionally to the laser wavenumber, resulting in an increasing observed intensity of Raman scattering with decreasing laser wavelength.

Although Raman scattering depends on effects such as polarizability, the empirically determined cross section σ_j is often used in analytical applications to relate to the Raman scattering intensity. The magnitude of Raman scattering cross section σ_j is related to $\delta\alpha/\delta Q_j$ as further described in the literature.[3] Equation (8) resulted from these theories. Equation (9) shows the relation between Raman scattering intensity I_R, the incident laser intensity I_0, Raman cross section σ_j, the number density of scatterers D and the path length of the laser in the sample dz.

$$I_R = I_0 \, \sigma_j \, D \, dz \qquad (9)$$

Equation (9) indicates that the scattering intensity is proportional to all parameters mentioned. In addition, the Raman cross section σ_j is proportional to the probability that an incident photon undergoes Raman scattering to yield a photon with a specific Raman shift.

The classical theory of Raman scattering does not fully account for the processes involved in resonance Raman scattering. Theories applying quantum mechanical treatment give a better understanding of resonance enhancement, e.g. Schrader's book[4] provides a good overview of these theories. However, resonance Raman scattering is addressed only briefly in this chapter, as it represents a minor aspect of the present thesis.

Resonance Raman scattering can occur when the energy of the laser line coincides with an electronic transition $E_0 \rightarrow E_1$ of a molecule as depicted in Figure 1-1 (e.g. for Stokes resonance Raman scattering). In comparison to Stokes Raman scattering certain vibrational modes are significantly enhanced in resonance Raman scattering due to an improved Raman scattering cross-section of the vibration.[5, 6] The scattering enhancement in resonance conditions often has an order of $10^3 – 10^4$ and can be up to 10^6. Since scattering efficiency from each vibronic level is not equal to the efficiency of absorption, the greatest resonance scattering intensity usually cannot be obtained at the maximum absorbance but at the lower energy side of an absorption band.[7]

1.1.2 State-of-the-art in Raman spectroscopic detection

In 1928, C.V. Raman and K.S. Krishnan[8] reported the experimental discovery of inelastically scattered light on molecules for the first time.[8] Since then, the number of applications and instrumentations in Raman spectroscopy (RS) has expanded considerably due to important developments in laser technology, optics, spectrographs

and information electronics with a focus on charge-coupled devices and computers.[2] However, the number of Raman spectroscopic detection systems for online coupling with an LC is still limited. This chapter will address the current state of research focusing on the benefits and challenges applying Raman detection for structural identification and the developments in flow cell design.

In 1981, M. D'Orazio and U. Schimpf[9] reported Raman spectroscopic detection of azoxybenzene derivatives after normal phase chromatographic separation. Carbon tetrachloride (CCl_4) with small amounts of ethanol was used as the eluent. The authors took into consideration that CCl_4 leads to only a few bands due to its high symmetry and small molecule size. Thus, CCl_4 is less likely to obscure sample bands when applying Raman detection. In addition, two excitation wavelengths were used to study the azoxybenzene derivatives at near-resonance and off-resonance conditions. Structural isomers were identified by comparing their off-resonance and near-resonance spectra. A stronger increase in the bands in the near-resonance spectra due to the vibronic coupling of molecular vibrations and electronic transitions in one of the isomers indicated slight differences in the chemical structure and resulted in the identification of both isomers.[9] However, resonance enhancement cannot be applied universally for an existing spectroscopic set-up, as it depends on the laser line matching an electronic transition of the target molecule.

In 1983, K. Iriyama and Y. Ozaki[10] detected the hemoproteins cytochrome c and myoglobin at resonance conditions in a flow cell connected to the high-performance liquid chromatography (HPLC) effluent. The authors used a stopped flow and an acquisition time of 4.5 min to obtain spectra of both hemoproteins. The authors pointed out that Raman detection after separation by HPLC can be applied non-destructively, and no special interface is required for coupling. In addition, Raman detection is highly compatible with water.[7, 10]

In 1991, R. Sheng et al.[11] analyzed purine bases with an online-coupling of reversed phase chromatography and surface-enhanced Raman spectroscopy (SERS). The effluent of the HPLC was mixed with silver sol prior to SERS detection in a glass capillary. SERS was applied to overcome the inherently low sensitivity of Raman spectroscopy in comparison to e.g. infrared spectroscopy. However, memory effects at the surface of the glass capillary revealed challenges in the use of online SERS detection.[11] Furthermore, SERS and RRS are often not suitable for quantitative analysis and highly specific as their enhancement effects are strongly related to the chromophores of the target molecules.[7, 12]

In 1996, T.D. Nguyen Hong et al.[13] reported the online coupling of HPLC and RS by employing a stainless steel capillary with a highly polished inner surface as detection cell. Toluene and naphthalene were analyzed within an acetonitrile water mixture equal to the mobile phase. A limit of detection (LOD) of 9.6 µg toluene injected on column could be achieved with their set-up. The authors pointed out that in comparison to UV detection the major advantage of Raman spectroscopy is the ability to reliably distinguish co-eluted components based on their unique Raman spectral pattern which

allows for structural identification.[13] In addition, Raman spectroscopy offers the opportunity to detect and quantify molecules without chromophores which can hardly be detected by UV absorption detection.[14]

While most of the earlier works combined conventional flow cells or glass / stainless steel capillaries with improved Raman scattering conditions such as SERS or resonance enhancement, latter works focused more on signal enhancement within the detection cell using capillary optics.

The principal of applying capillary optics for Raman signal intensity enhancement originates from Walrafen and Stone[15] on fused-quartz capillaries in 1972. A Raman signal intensity enhancement of approximately 10^2 – 10^3 could be reached by applying 10 – 25 meter long fused-quartz capillaries filled with benzene or tetrachloroethylene as detection cell.[15] However, the applicability of fused-quartz capillaries for Raman signal enhancement was limited to liquids with a refractive index higher than quartz (1.46).[16] In the late 1990's and early 2000's, Altkorn et al.[17-19] conducted fundamental studies on Teflon AF 2400 capillaries, which is an amorphous fluoropolymer with a refractive index of 1.29.[12, 18-20] Since most common LC eluents, e.g. water (1.3352), methanol (1.3305), and acetonitrile (1.3447),[21, 22] have higher refractive indices than Teflon AF 2400, total internal reflection of light can occur at the critical angle at the surface between the capillary cladding and the liquid core.[23] Thus, the liquid core waveguide (LCW) extends the excitation path length for Raman scattering, thereby enhancing the Raman signal intensity.[14, 24] Altkorn et al.[17-19] examined how variations in fiber length, inner diameter, laser wavelength, and detection geometry affect Raman signal intensity and signal-to-noise ratio (SNR).

In 1999, Dijkstra et al.[20] and Marquardt et al.[12] both published studies on the online coupling of HPLC and RS by applying an LCW of Teflon AF 2400 as detection cell. Dijkstra et al. investigated different aromatic nitro substances, which were separated by reversed-phase chromatography with a mixture of methanol and phosphate buffer as eluent. LODs were estimated to be 10 µg/mL (4-nitroaniline), 50 µg/mL (4-nitrophenol), 250 µg/mL (2,4-dinitrophenol), and 500 µg/mL (nitrobenzene) when using large volume injections of 500 µL.[20] Marquardt et al.[12] analyzed a mixture of four different alcohols in purely aqueous reversed-phase chromatography with a cyanopropyl stationary phase. In addition, spectra of ten different alcohols obtained sequentially from the individual standard solutions could be clearly distinguished from each other based on their Raman spectra. The authors determined the LOD and enhancement effect of the LCW based on the SNR of 817 cm^{-1} in phase C-C-O stretching mode of isopropyl alcohol diluted in water. The Raman spectrum of 1 % isopropyl alcohol in water in a vial resulted in a SNR of 3.2, whereas a SNR of 4.1 was reached for 10 ppm isopropyl alcohol in water within the LCW (1.9 µL internal volume). Thus, an enhancement in the detection of isopropyl alcohol diluted in water of more than 1,000 folds could be reached by using an LCW for Raman detection. The LOD of the LCW used was determined to be 2 ppm of isopropyl alcohol in water.[12]

In 2001, Dijkstra et al.[25] published the analysis of different nucleotides with HPLC-Raman coupling. The optimum length of the LCW and the relative enhancement factor of the LCW over the wavenumber range were discussed at different excitation wavelengths. The authors concluded that the relative enhancement factor of the LCW increases with decreasing wavelength. In addition, the relative enhancement factor of the LCW is more constant over the wavenumber range for shorter wavelengths. Furthermore, the length of the LCW can be increased with decreasing wavelength because of a lower attenuation due to inner surface defects or high-overtone vibrational band absorption of the core liquid in the near-infrared range.[25] However, peak widths and band broadening must be considered when increasing the length of the LCW for detection.[20] In addition, aqueous separation modes such as ion exchange chromatography or size exclusion chromatography are desirable as the Raman band of water does not obscure spectral features of the analytes in comparison to organic solvents.[25] Moreover, large volume injections and stopped flow measurements are options to improve the detectability of various analytes.[20, 25] Further improvements in the Raman spectroscopic detection can be reached by higher laser powers which is also in accordance with equations (8) and (9).[2, 20]

A special case of capillary optics is the vertical flow technique (VFT) developed by H. Hiramatsu and T. Saito[26] in 2013. In the VFT, the laser light is focused into a laminar flow column of liquid which is surrounded by air. The light is propagated by total internal reflection at the liquid-air-interface. Considering the refractive indices of air (1.00) and water (1.33), the critical angle at the air-water interface can be calculated to be 49°.[26] In comparison the critical angle at the Teflon AF 2400-water interface is 75.9°.[16] Therefore, VFT allows more efficient collection of Raman scattered light due to the lower critical angle. The VFT was applied as detection cell for online coupling HPLC and RS by Y.-H. Lo and H. Hiramatsu[27] in 2020 and by Y.-S. Chen and H. Hiramatsu[28] in 2025. However, from an occupational safety perspective, working with a capillary-guided flow profile is preferable to a laminar flow profile surrounded by air when using common HPLC eluents such as acetonitrile or methanol.

Y.-H. Lo and H. Hiramatsu analyzed the structural isomers ortho-, meta- and para-methoxyphenol and achieved LODs between 1.2 – 4.1 mM.[27] Y.-S. Chen and H. Hiramatsu reported LODs between 61 – 81 µg/mL for different mono- and disaccharides separated by hydrophilic interaction chromatography (HILIC).[28] Apparently, comparing the detection limit between different studies is not straightforward, as different units are used to report the LOD ranging from mass or molar concentrations to percentages or masses. Table 1-1 provides an overview of the detection limits achieved with capillaries as detection cells, highlighting the kind of detection cell, the substances analyzed, and the laser conditions used. For better comparability, the LOD was calculated as injected mass on column to account for differences in the injected volumes. The injected mass on column means concentration of the injected solution multiplied by the injected volume.

Table 1-1: Limits of detection (LOD) determined in various studies by applying online-coupled HPLC-Raman with a stainless steel capillary (SSC), a liquid core waveguide (LCW) or vertical flow technique (VFT) as detection cell.

Technique	Substance	Laser conditions	LOD (as reported)	LOD (injected mass on column) [µg]	Reference
SSC	toluene	514.5 nm, 1000 mW	9.6 µg	9.6	13
LCW	4-nitroaniline	514.5 nm, ~40 mW	10 µg/mL	5	20
LCW	isopropyl alcohol	785 nm, 60 mW	2 ppm	0.0158	12
LCW	caffeine	532 nm, 2000 mW	500 ng	0.5	16
VFT	o-methoxyphenol m-methoxyphenol p-methoxyphenol	785 nm, not specified	1.2 mM 2.7 mM 4.1 mM	149 335 509	27
LCW	sucrose	532 nm, 600 mW	120 µg	120	14*
VFT	fructose glucose sucrose maltose trehalose	532 nm, not specified	61 µg/mL 68 µg/mL 74 µg/mL 68 µg/mL 81 µg/mL	61 68 74 68 81	28

* more details are provided in chapter 2 of this thesis

When comparing the LODs of isopropyl alcohol in an LCW[12] and toluene in a polished stain-less steel capillary,[13] it becomes apparent that the LCW significantly improves the detection limit. The LOD for isopropyl alcohol is approximately 50 times lower than for toluene despite using higher wavelength and significantly lower laser power in the LCW. This highlights the significant signal intensity enhancement resulting from total internal reflection in the LCW compared to diffuse reflection in the polished metal capillary. Most dissolved solutes such as sugars[14, 28] or the methoxyphenol isomers[27] achieve LODs approximately between 60 – 510 µg injected on column which is significantly higher than the LOD achieved for a neat liquid such as isopropyl alcohol (0.0158 µg) diluted in water. On the other hand, dissolved solutes such as 4-nitroaniline or caffeine could be detected in the lower microgram range (0.5 – 5 µg) either due to favorable scattering properties of the substance detected[20] or due to laser powers applied in the LCW.[16]

In comparison to other techniques coupled with LC such as refractive index detection (RI),[29] evaporative light scattering (ELSD),[30] and mass spectrometry (MS)[31], the LOD

achieved with Raman detection is significantly higher. An LOD of 74 µg could be achieved for sucrose by coupling HILIC with Raman detection.[28] Similar chromatographic conditions coupled with other detectors such as RI, ELSD, and MS achieved detection limits in the low microgram to sub-microgram range with LODs of 3.2 µg, 0.34 µg, and 0.05 µg, respectively,[29-31] highlighting the inherently low sensitivity of Raman spectroscopic detection. On the other hand, RS provides additional spectral information that can be used to unambiguously identify compounds that might co-elute.[13]

In summary, various analytes have been analyzed with Raman spectroscopic detection after LC ranging from neat liquids such as alcohols, toluene[13] or carbon tetrachloride[9] to various solutes such as nitroaromatics[20] or azobenzene,[9] nucleotides,[32] sugars,[28] and hemoproteins.[10] However, in most studies artificial mixtures or pure compounds were analyzed rather than real samples. The detection and quantification of different sugars in native honey[28] is the only example of a real sample analyzed by Raman spectroscopic detection for liquid chromatography.

1.2 Biopharmaceuticals

Raman spectroscopy can provide insights into the structure of molecules. Since the present thesis focusses on the analysis of proteins and biopharmaceutical products, chapter 1.2 highlights main aspects of the native structure of proteins and its relevance in functionality and activity. In addition, biopharmaceutical development of therapeutic proteins is presented in detail giving insights into the biopharmaceutical production, formulation considerations and the importance of biopharmaceutics in disease treatment and prevention.

1.2.1 Proteins

1.2.1.1 The native structure

Natural proteins mainly assemble from the 20 canonical amino acids. The various amino acids are covalently linked by an amide bond, the so-called peptide bond, which builds the backbone of the three-dimensional structure of a protein.[33] The three-dimensional structure of a protein arises from its primary structure, i.e. its amino acid sequence.[34]

In Figure 1-2, two consecutive peptide bonds within the polypeptide chain are depicted. The peptide bond is planar due to steric limitations (plane is shown as grey rectangle). However, rotations are possible along the C_α-C (ψ-angle) and the N-C_α bonds (φ-angle) between the different peptide bonds enabling folding of the polypeptide chain.[35]

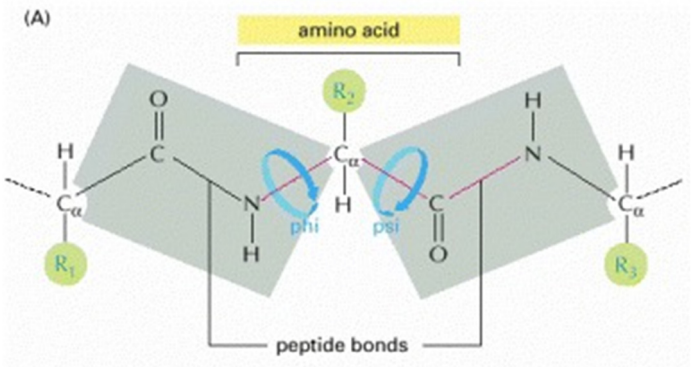

Figure 1-2: Rotational angles within the polypeptide chain. Adapted from Alberts et al.[35]

Folding into its native structure is a spontaneous process which is supported by various intra- and intermolecular interactions such as hydrogen-bonding, ionic, van der Waals and hydrophobic interactions.[34]

Hydrogen-bonding between the C=O of one peptide bond and the N-H group of another peptide bond results in sections of regular, repeating folding patterns.[35] The most common secondary structural elements in proteins include α-helices, β-sheets (both regular folding) and random coils (irregular folding).[36]

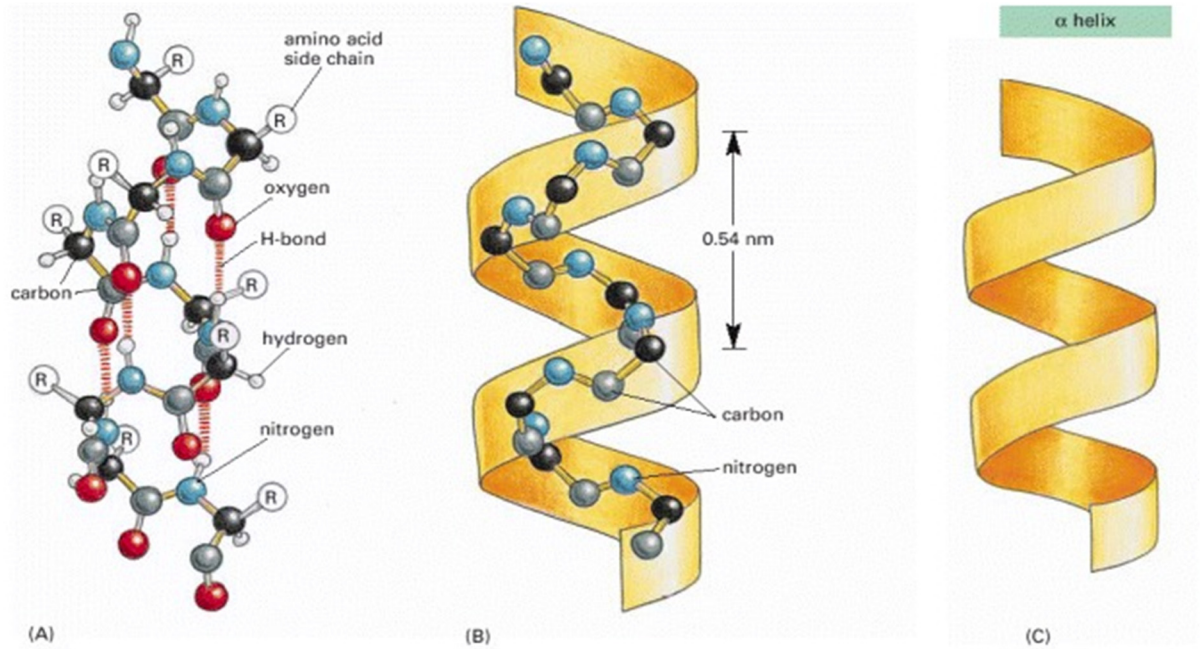

Figure 1-3: Secondary structural elements in proteins: α-helix. Adapted from Alberts et al.[35]

α-helices are formed by hydrogen-bonding interactions between the carbonyl oxygen and the amino nitrogen of the i^{th} and $i+4^{th}$ amino acid along the peptide backbone. The amino acid side chains (R in Figure 1-3) are oriented towards the outside of the helix.[36] Figure 1-3 demonstrates the α-helix conformation.

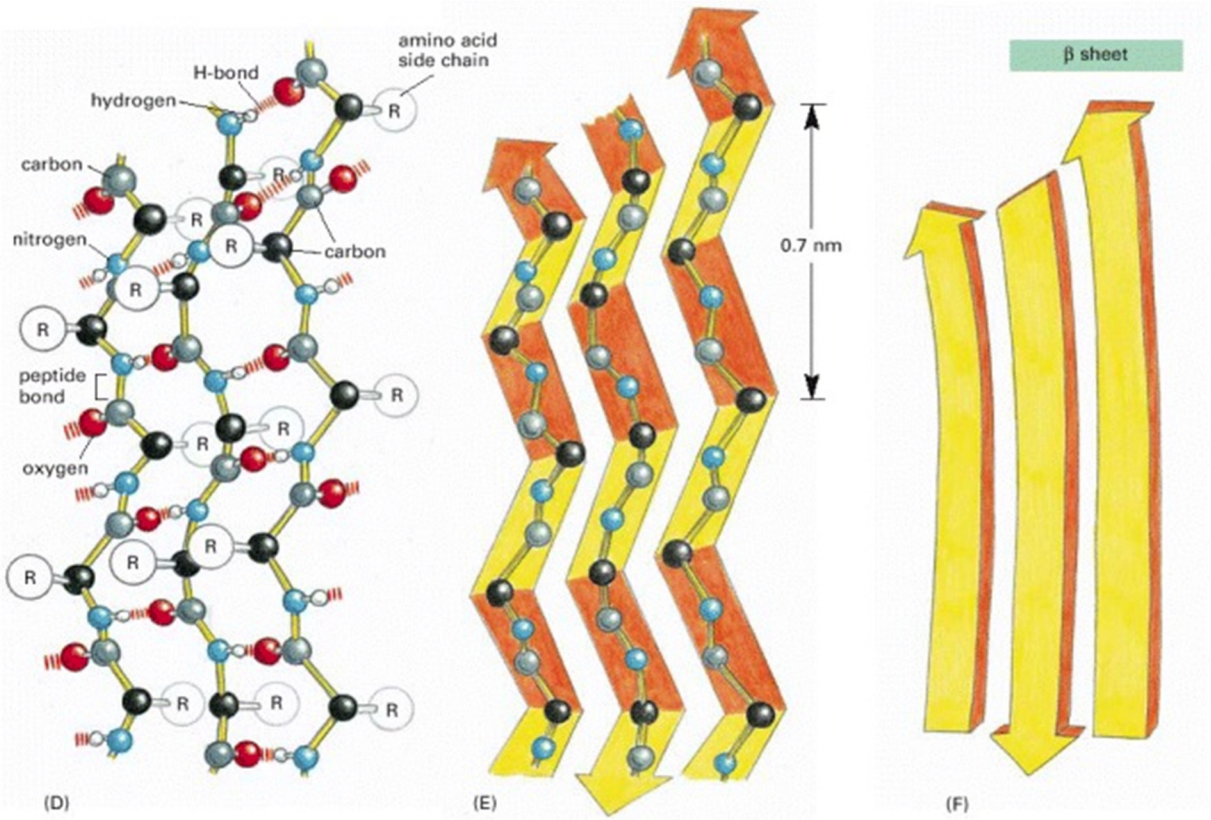

Figure 1-4: Secondary structural elements in proteins: β-sheet. Adapted from Alberts et al.[35]

The β-sheet structures result from hydrogen-bonding between different neighboring strands of the polypeptide backbone that are oriented either parallel or antiparallel to each other.[33, 35] In an antiparallel β-sheet, the polypeptide chains run in opposite directions, alternating between C-to-N terminal and N-to-C terminal. In contrast, in a parallel β-sheet, all strands run in the same direction.[37] In β-sheet conformation the amino acid side chains (R in Figure 1-4) are alternately oriented above or below the plane of the β-sheet as demonstrated in Figure 1-4 for the antiparallel β-sheet.[33, 35] Other secondary structures include the π-helix and the 3_{10}-helix,[38] and β-turns.[33] Loops and β-turns can connect other secondary structural elements by changing the direction of the polypeptide chain and thereby allowing to create a more compact three-dimensional structure.[39]

Various interactions between the amino acid side chains such as hydrophobic interaction, hydrogen-bonding, electrostatic forces and the formation of covalent disulfide bonds result in the formation of the tertiary structure of the protein.[37] Thus, the tertiary structure derives from the three-dimensional arrangement of various secondary structural elements.[39] The different properties of the amino acid side chains, e.g. polar or non-polar, positively or negatively charged, influence the individual conformation of each protein. Furthermore, hydrophobic interactions play a major role in the folding process as native proteins have hydrophobic cores in aqueous media. Thus, non-polar amino acid residues will be orientated towards the hydrophobic core whereas polar or charged amino acid side chains are more likely to be at the hydrophilic surface of the native protein.[35]

Various proteins, e.g. hemoglobin, assemble from more than one polypeptide chain. The quaternary structure is given by the arrangement of several subunits, i.e. the individual polypeptide chains, to form the native conformation of the protein.[37]

According to their shape and solubility proteins can be differentiated into three major classes: fibrous, globular and membrane proteins. Fibrous and membrane proteins are generally insoluble in aqueous media. In contrast, globular proteins are highly soluble in aqueous media. The shape of fibrous proteins is rod-like whereas globular proteins have a nearly spherical shape.[37]

1.2.1.2 Functionality and activity

Proteins are versatile macromolecules that fulfill essential and highly diverse functions within the human body. For example, they act as catalysts for biochemical reactions, form receptors and channels in membranes, and facilitate the transport of a wide variety of molecules either intracellular or through the whole body.[40]

The function of a protein is determined by its distinct three-dimensional structure.[39] The native conformation is important for proteins to serve various physiologically relevant functions. A misfolding of their native conformation can result in protein aggregation which can create a pathogenic form. For example, neurodegenerative diseases such as Alzheimer's and Parkinson’s disease are characterized by the misfolding and aggregation of a specific protein.[41] Another example is the autosomal recessive

disease cystic fibrosis where affected individuals have a mutation in the CFTR gene leading to misfolding and consequent degradation or dysfunction/altered expression of the CFTR protein.[42]

The conformation of proteins is highly specific and conserved, meaning that certain amino acid residues are precisely positioned within the three-dimensional structure to enable functionality at the active sites. This allows for catalytical activity of enzymes or high-affinity binding of targeted molecules.[39] For example, antigen-antibody interactions often lead to conformational changes in the contact surfaces of both the antigen and antibody.[43] Furthermore, hemoglobin experiences distinct conformational changes in the tertiary structure upon binding of ligands such as oxygen. These structural changes also affect the unliganded subunits and thus increase their affinity to bind oxygen. This phenomenon is known as allosteric activation and highlights the importance of the higher-order structure for functionality.[44]

In addition to the conformation, post-translational modifications (PTMs) like glycosylation, phosphorylation, and acetylation affect the biological structure, function, and activity of proteins.[45] The antibody-dependent cellular cytotoxicity (ADCC) potency depends on the glycosylation pattern of a monoclonal antibody.[39] For example, the lack of fucose in the glycosylation pattern of the fragment crystallizable (F_c) region can lead to increased binding of FcγRIIIa receptor, which results in an enhanced immune response against cancer cells based on ADCC and antibody-dependent cellular phagocytosis. Therefore, strategies such as glycoengineering are used in the development of therapeutic proteins to actively influence pharmacokinetics and pharmacodynamics to achieve an optimal function of the therapeutic proteins.[46]

1.2.2 Biopharmaceutical products

1.2.2.1 Biotechnological production

Proteins are usually produced biologically or biotechnologically in living cells or organisms. The first protein therapeutics, e.g. insulin for the treatment of diabetes mellitus, had to be extracted from animals' pancreases.[47] Recombinant DNA technology enabled a break-through in the production of therapeutic proteins since it has several advantages over isolation of non-recombinant proteins. The gene sequence can be modified using recombinant technology to achieve improved specificity or function, which can lead to highly specific activity and a decreased immunological response for recombinant proteins through targeted expression of a desired gene.[40] Furthermore, the production of recombinant proteins is more efficient and offers better scalability, as it does not rely on material from living organisms. On the one hand, this avoids the risk of transmissible viral or prion diseases and, on the other hand, enables a significantly higher production volume.[40, 46]

The production of therapeutic proteins by recombinant DNA technology is a multistep process, starting with the selection of a target gene.[48] Different approaches are applied to discover and identify potential protein therapeutics. Certain target proteins can be

isolated and purified from an organism or bodily fluids. In addition, hybridoma technique and transgenic technology are used to screen for new antibody candidates.[49] *De novo* protein design enables the discovery and creation of proteins and structures beyond those found in nature and encoded by evolution in the genome.[50] All these approaches can result in the identification of a gene of interest which is used for biotechnological production.

Today, most protein therapeutics are produced by recombinant DNA technology in a diverse range of organisms including bacteria, yeast, fungi, mammalian cells, insect cells, and transgenic animals and plants.[40, 51] The expression system has an influence on the biological activity of the proteins as the various systems result in different PTMs of the protein. In particular, the glycosylation pattern significantly influences the activity, half-life, and immunogenicity of the therapeutic protein *in vivo*.[40] *E. coli* is among the most important production systems for non-glycosylated therapeutic proteins such as insulin. Mammalian cells are preferred if PTMs such as glycosylation sites are required to prevent immunogenic responses and ensure the stability and activity of the therapeutic proteins.[48] Chinese hamster ovary (CHO) cell lines are among the most commonly employed mammalian cell lines, e.g. for the production of many monoclonal antibodies.[52]

Depending on the cell line, i.e. prokaryotic or eukaryotic, different techniques are used to either transform the target gene into prokaryotic cells or transfect it into eukaryotic cells. In the case of bacterial cells, the target gene is inserted into an expression vector, followed by the transformation of the vector into the prokaryotic cells.[48] In the case of mammalian cell lines, the gene of interest can be transfected either using a viral vector, (physico-)chemical methods or hybrid strategies of both techniques. After transfection, high-productivity clones are selected from the transfected cells to maximize the production yields in the growth stage.[52] The clonal cells are then cultivated in growth medium to achieve high production yields of the recombinant protein, which is finally isolated and purified from the culture medium.[48] The growth in cell culture conditions is referred to as upstream processing, whereas the harvest and purification steps are part of the downstream processing.[53]

1.2.2.2 Formulation considerations

Proteins are sensitive to environmental influences such as thermal stress or shear stress, and changes in pH which can occur during the production process, shelf life or transportation. Thus, proteins are prone to physical or chemical instability. Physical instability causes denaturation of the proteins and the formation of aggegrates.[54] Chemical instability leads to, e.g. oxidation, reduction, deamidation, hydrolysis, fragmentation, isomerization, formation of additional acidic or basic variants, Maillard reaction in glycosylated proteins, and C-terminal clipping.[55]

In addition, the high molecular weight of proteins leads to a reduced permeability in mucosal or cell membranes, and skin. Thus, injections are the most important route of administration including intravenous, intramuscular and subcutaneous injections.[56]

Proteins are usually formulated as liquid or lyophilized products to create an acceptable shelf life while preserving the activity and minimizing the potential for adverse immune responses. Especially monoclonal antibodies have EC50 values 10 – 1,000 times higher than for other proteins, requiring antibodies to be formulated at high concentrations to reduce the dose volume. However, high concentrations increase the tendency of proteins to aggregate.[54] Therefore, formulation excipients play a crucial role in stabilizing antibodies in solution, for example by preventing their aggregation.[57] Sugars and polyols, amino acids, antioxidants, preservatives, surfactants, salts and buffers have proven to stabilize antibodies and to facilitate their administration. Each of these excipients has a certain function. Table 1-2 provides an overview of the functions of different excipient classes and gives some examples of commonly used substances.[58]

Table 1-2: Common excipients in biopharmaceutical products and their function adapted from D. J. A. Crommelin et al.[58]

Excipient class	Function	Examples
amino acids	stabilization, viscosity reduction, tonicity, pH control, bulking agent for freeze-dried products	arginine, glycine, histidine, lysine, proline
antioxidants	oxidation prevention	methionine, sodium edetate
buffers	pH control, tonicity	histidine, phosphate, acetate, citrate, succinate
preservatives	bacterial growth prevention	m-cresol, benzyl alcohol, phenol
salts	tonicity, stabilization, viscosity reduction	sodium chloride
sugars, polyols	tonicity, stabilization, cryoprotection; for freeze-dried products: lyoprotection, bulking agent, reconstitution improvement	sucrose, trehalose, mannitol, sorbitol
surfactants	adsorption prevention, solubilization, stabilization, reconstitution improvement	polysorbate 20, polysorbate 80, poloxamer 188

Buffers and amino acids can stabilize the pH and ionic strength of the solution, which is important to enhance the solubility of the protein. The pH affects the net charge of a protein, thereby influencing its solubility. Surfactants are commonly used to prevent adsorption of protein to hydrophobic surfaces. On the one hand, adsorption reduces the total amount of active ingredient and on the other hand, it may promote protein aggregation due to partial unfolding caused by the adsorption to surfaces. Surfactants

prevent protein adsorption as they adhere to hydrophobic surfaces and expose their hydrophilic groups. Aggregation due to high concentration or conformational instability can be prevented by adding sugars, adjusting the pH and ionic strength. However, it is important to note that only non-reducing sugars should be used, since reducing sugars may induce chemical instability through the Maillard reaction. In addition, sugars and polyols are used as lyo- and cryoprotectors. Antioxidants are added to prevent physical instability of the protein caused by oxidation of specific amino acids. Preservatives should inhibit microbial growth in the biopharmaceutical product in multi-dose containers. Parenteral administration requires an adequate tonicity of the product. Therefore, buffers, amino acids, sugars and polyols, and salts are added to adjust the tonicity of the product.[58] All these surrogates must be separated from the therapeutic proteins to obtain Raman spectra solely of their structure.

1.2.3 Therapeutic Proteins: Importance and treatment options

Whereas therapeutic strategies in the 20th century were predominantly based on small-molecule drugs, the beginning of the 21st century marked the era of a new class of pharmaceuticals in disease treatment: biologics / biopharmaceuticals. Biologics are highly complex molecules which are produced using biological or biotechnological processes, involving living cells or organisms. This distinguishes them fundamentally from small-molecule drugs, which can be synthesized through conventional chemical methods. Biologics are a highly heterogeneous class of therapeutics, including for example peptides, proteins, as well as cells and tissues.

In 1982, the rise of modern therapeutic proteins began with the FDA approval of Humulin (insulin) – the first recombinant, protein-based therapeutic. Approximately 40 years later, in 2021, the FDA approved the 100th unique monoclonal antibody.[46] Recombinant antibodies and their derivates, i.e. monoclonal antibodies, antibody fusion proteins, nanobodies, and antibody-drug conjugates, account for more than 40 % of all biopharmaceutical products approved in Germany and for 64 % of the candidates in the development pipeline, highlighting their importance in the biopharmaceutical sector.[59] Current market projections for 2025 underline the increasing importance of biologics in disease treatment, since 8 of the 10 top-selling drugs worldwide are biopharmaceutical drugs. Among these forecasted top-selling biologics are four monoclonal antibodies as well as four peptide-based drug products.[60] In 2024, biopharmaceuticals accounted for 64 % of all new drug approvals in the European Union and achieved a 35 % share of the total pharmaceutical market with a revenue of around 21.4 billion €.[59]

The development of biopharmaceutical products such as therapeutic proteins led to diverse treatment options for patients suffering from autoimmune diseases,[61, 62] cancer,[63, 64] hemostasis disorders,[65] neurological disorders,[66] diabetes mellitus[46] or infectious diseases.[67] Leader et al.[40] developed a pharmacological classification for therapeutic proteins based on their function as depicted in Figure 1-5. Proteins can be divided into four main categories: enzymatic / regulatory activity, special targeting activity, protein vaccines, and protein diagnostics.[40]

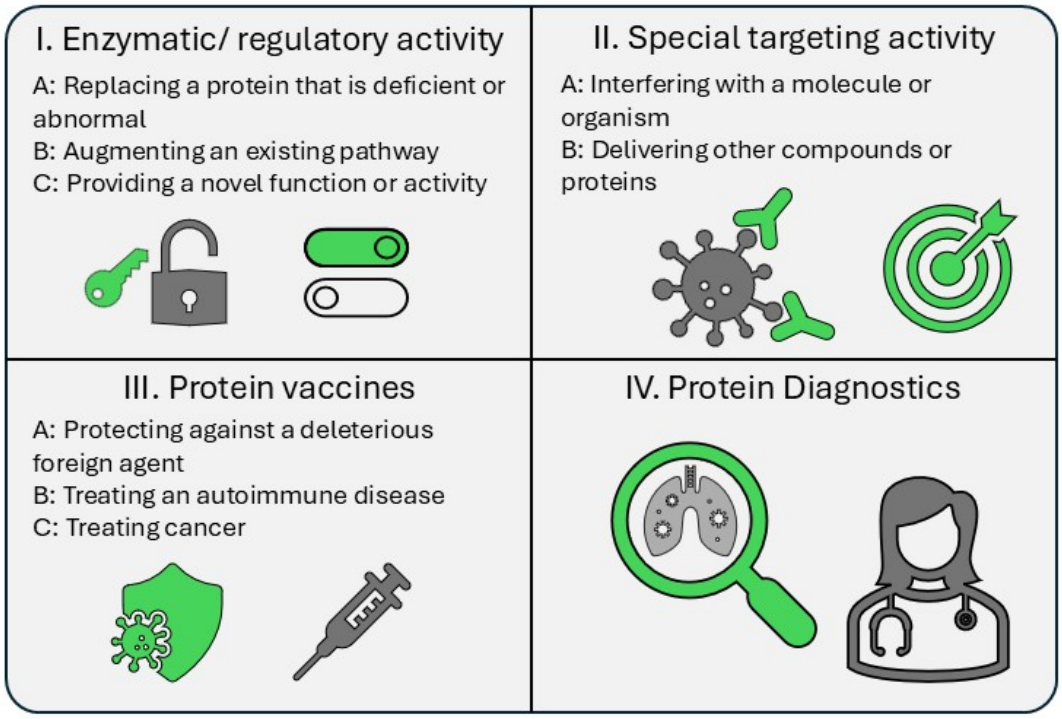

Figure 1-5: Overview of the pharmacological classification of therapeutic proteins according to Leader et al.[40]

Proteins of the first group fulfill an enzymatic or regulatory activity in the body. Depending on the subclasses, these proteins are divided into therapeutic proteins that replace a deficient or abnormal protein within the body, proteins that augment an existing pathway or they provide a novel function or activity.[40] The application of insulin for the treatment of diabetes mellitus and providing exogenous lactase in patients suffering from lactose intolerance are examples of enzymatic activity from Group IA.[68, 69] Proteins of the second group deliver compounds and interfere with a molecule or organism. Monoclonal antibodies and antibody-drug conjugates used in cancer therapy are among this group.[40] Monoclonal antibodies effectively interfere with the processes of the immune system with their targeted binding properties, e.g. by inducing ADCC.[70] Antibody-drug conjugates can target tumor cells and deliver conjugated cytotoxic agents to these cells which interrupt cell proliferation.[71] Protein vaccines are designed to protect against infectious diseases or toxins. For example, recombinant proteins can be used to improve immunogenicity by covalently binding to a specific antigen.[72] Another approach involves using recombinantly produced capsid proteins, which are assembled into virus-like particles, to create a non-infectious vaccine.[73] Protein diagnostics can be used for *in vivo* or *in vitro* diagnostics of various diseases. For example, monoclonal antibodies conjugated with radioactive isotope ^{111}indium or with a fluorescent dye such as IRDye800CW enable targeted binding to tumor cells. In combination with imaging techniques such as computer-assisted tomography and magnetic resonance imaging, protein diagnostics can aid in diagnosis and staging of cancer.[74] Thus, therapeutic proteins are a versatile class of active

ingredients that can be effective in the treatment and curing of various conditions and diseases.

1.3 Protein characterization

1.3.1 Benefits and challenges of Raman spectroscopy for protein analysis

In general, typical benefits, e.g. non-destructive and label free application, high compatibility with aqueous or saline media, and identification based on vibrational modes and challenges such as fluorescence interference or low sensitivity also apply to the analysis of proteins. However, this chapter focuses on aspects of analyzing proteins using Raman spectroscopy and biochromatography.

RS is sensitive to the conformation of a protein and therefore certain marker bands of the tertiary and particularly the secondary structure are often used to analyze changes in protein structure related to folding/ unfolding[75] or especially in the formation of aggregates.[41, 76-79] Besides mechanistic studies employed to understand the processes involved in protein folding and aggregation, other studies used RS to examine aggregates, i.e. amyloid fibrils, in various tissue samples.[80-82] Therefore, RS is beneficial in the analysis of the three-dimensional structure of proteins. In Figure 1-6 some of the characteristic parts in a protein Raman spectrum are highlighted which provide information on the secondary and tertiary structure of a protein.

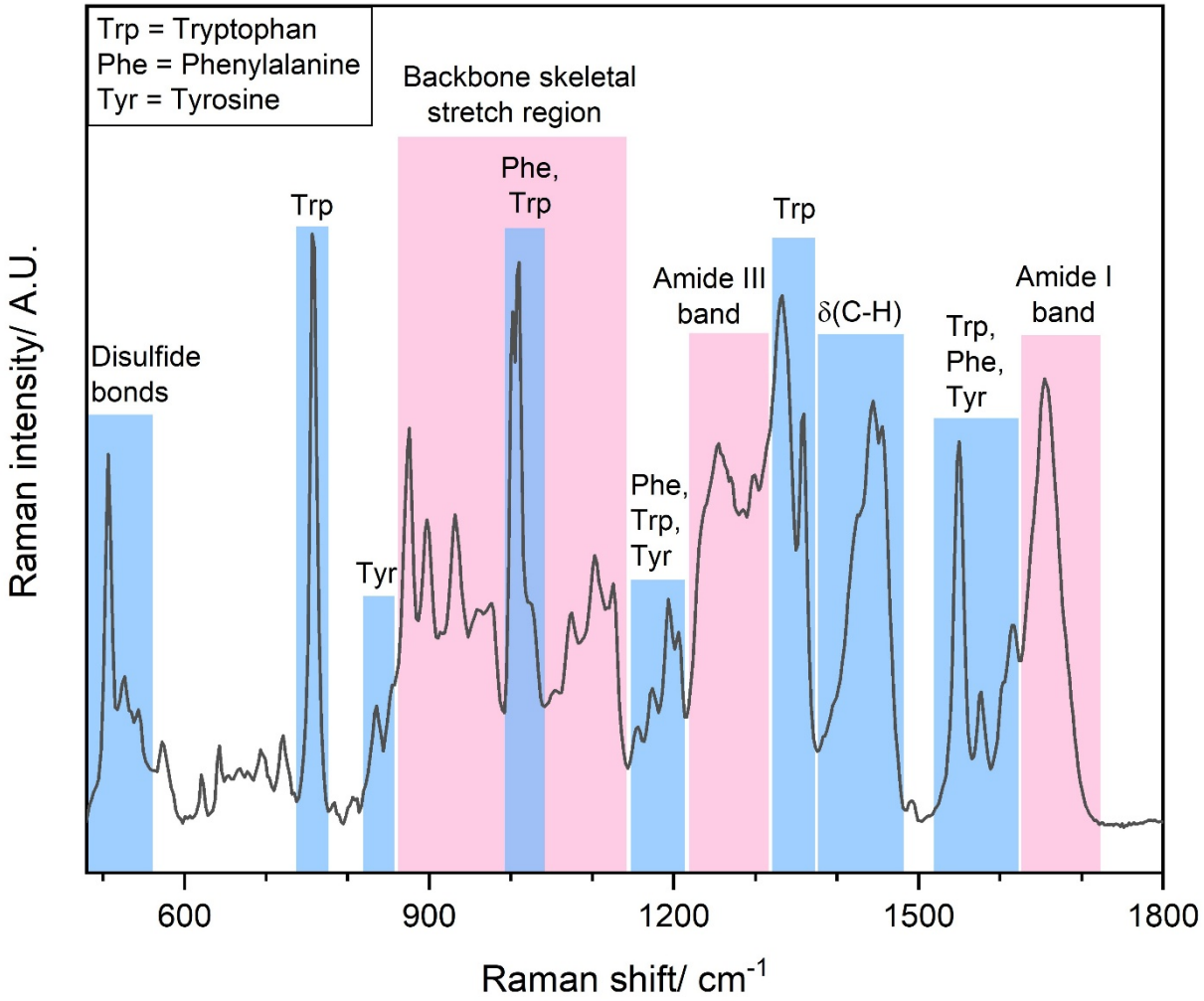

Figure 1-6: Raman spectrum of hen egg white lysozyme adapted from J. Thissen.[83] Information related to the secondary structure (pink) and to the tertiary structure (blue) of the protein is highlighted and can be found in the literature.[84, 85]

For example, the Amide I band results mainly from the stretching mode of the carbonyl group of the peptide bond. The three-dimensional orientation and hydrogen bonding strength of the polypeptide chain affect the vibrational frequency giving rise to different Raman shifts for structural elements such as α-helix, random coil or β-sheet due to different dihedral angles of the backbone conformation.[86, 87] The vibrational modes of the secondary structural elements commonly overlap in Amide I band. Therefore, various conformations can result in different maximum position of Amide I band.[85] In addition, the shape of the Amide III band is influenced by secondary structures in protein conformation.[87] The α-helices contribute to the Amide III band at a Raman shift of 1,270 – 1,300 cm^{-1}, while β-sheet or random structure correspond to Raman shifts of 1,230 – 1,240 cm^{-1} and 1,240 – 1,250 cm^{-1}, respectively.[87] In the backbone skeletal stretch region, the positions of C_α-C or N-C_α-C stretching modes are influenced as well by secondary structure. While α-helical structure leads to bands at ~900 cm^{-1} and between 930 – 950 cm^{-1}, bands for β-sheet rich proteins can be observed between 960 – 980 cm^{-1}.[77, 78, 86, 87]

In addition, information on the tertiary structure can be gained especially by analyzing the different vibrations related to the aromatic amino acids tyrosine and tryptophan. The intensity ratio of the tyrosine fermi doublet I_{850}/I_{830} provides insights into the hydrogen bonding state between phenyl-OH group of tyrosine and solvent molecules. Changes in the microenvironment of tyrosine, e.g. due to aggregation, can be derived from this intensity ratio.[79] Furthermore, the tryptophan fermi doublet I_{1360}/I_{1340} is sensitive to the hydrophobicity of the surrounding environment of the indole ring, i.e. solvent or residues of other amino acids. The ratio increases if the hydrophobicity of the microenvironment increases.[88] These were examples to highlight the possibilities of RS to analyze the conformation of proteins. Further information on structural analysis of proteins applying Raman spectroscopy is summarized in various reviews.[85-87]

In quality assurance and evaluation, reliable and objective differentiation of spectra acquired by vibrational spectroscopy is challenging.[89] Despite qualification of differences, also quantification of changes in the Raman spectrum such as changes in the Amide I band can be demanding. Therefore, RS is commonly combined with chemometric tools for a more comprehensive and reliable data evaluation. Peak deconvolution based on band curve fitting can be applied to investigate the relative amounts of different secondary structures more in detail.[78, 79, 90] Furthermore, the combination of band curve fitting with partial least squares (PLS) regression modeling as a machine learning tool enabled accurate prediction of the secondary structural content for proteins.[91] Principal component analysis (PCA) can reveal variances between spectra, allowing three different monoclonal antibodies in three batches to be distinguished.[92] In another study, PCA could resolve spectral variances related to changes in the secondary and tertiary structure of an investigated protein due to varying formulation conditions.[93] Multivariate curve resolution alternating least squares (MCR-ALS) can resolve pure spectra of individual components in a multi-component system which can be applied to quantitate the amount of secondary structural elements based on Amide I band.[94]

In summary, RS provides a variety of selective information on the conformation of proteins, enabling the analysis of changes in the higher-order structure and differentiation of proteins according to their Raman spectra. Chemometric analysis tools offer further possibilities to analyze protein samples more in depth.

1.3.2 Biochromatography – Benefits and challenges in coupling with Raman spectroscopic detection

In biopharmaceutical development, comprehensive characterization of biotechnological or biological products (ICH Q6B) and stability testing (ICH Q5C) is required by regulatory authorities to obtain marketing authorization.[95, 96] Biochromatographic modes such as ion exchange chromatography (IEX), hydrophobic interaction chromatography (HIC), and size exclusion chromatography (SEC), can contribute to the comprehensive characterization and stability testing of biopharmaceuticals.[97] The following chapter outlines the properties of the different

chromatographic techniques focusing on commonly applied mobile phases and elution modes.

IEX enables separation of charge variants of monoclonal antibodies and their derivates. Degradation processes such as deamidation or isomerization can result in the formation of acidic or basic variants and thus, potentially impact stability and biological activity of the therapeutic proteins. The separation in IEX is based on electrostatic and ionic interactions of proteins with a charged stationary phase. Depending on the stationary phase, a distinction can be made between cation (acidic functional groups) and anion (basic functional groups) exchangers and further into weak and strong exchangers. Elution of the analytes is performed by an increase in ionic strength, a change in pH or a combination of both.[98] Protein separations are frequently performed with 2-(N-morpholino)ethanesulfonic acid (MES), phosphate or citrate buffers depending on the isoelectric point of the protein and the acid dissociation constant of the stationary phase material. Salt gradient elution is typically conducted with sodium or potassium chloride. pH elution usually requires a mix of different buffering species which include imidazole, triethylamine, diethylamine, ammonium hydroxide, piperazine or tris base.[99]

SEC can be applied to assess the molecular size of the monomeric protein as well as to quantify the content of potentially formed aggregates or fragments that are considered as a product-related impurity according to ICH Q6B.[95] While most separation techniques are based on partition chromatography, the separation in SEC is driven by the permeation of molecules into a porous stationary phase material. The stationary phase of modern analytical SEC columns consists of spherical porous particles with a controlled pore size. Proteins are separated based on their hydrodynamic radius as they diffuse into the pores of the stationary phase.[100] Biomolecules with a smaller hydrodynamic radius can diffuse in more and smaller sized pores and thus elute at higher elution volumes, whereas larger sized proteins elute at lower elution volumes as demonstrated in Figure 1-7.[101]

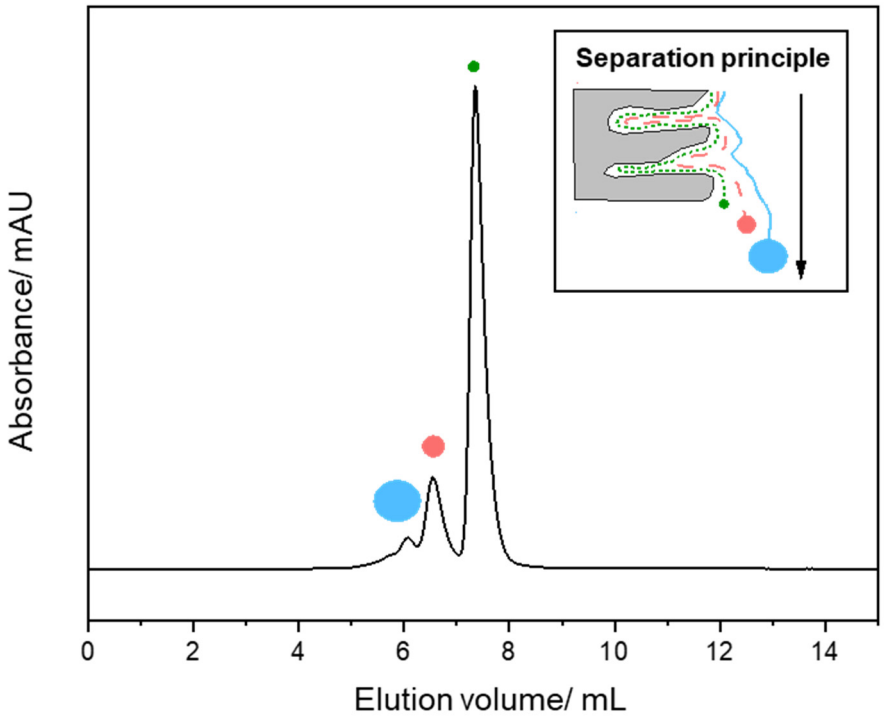

Figure 1-7: Separation principle of size exclusion chromatography adapted from J. Thissen.[83]

In an ideal setting, the separation should be driven by entropic processes without any adsorption to the stationary phase.[100, 102] However, electrostatic and hydrophobic interactions of proteins with the charged surface sites of the stationary phase are well described in the literature.[100, 102] These interactions can lead to shifts in the elution volume, peak asymmetry or peak tailing. Therefore, mobile phases with increased ionic strength of typically 50 – 200 mM are applied to reduce especially the electrostatic interactions of the proteins with the stationary phase material. Sodium or potassium chloride or sodium sulfate can improve the peak shape and thus are frequently added to the mobile phase at a concentration of 10 – 250 mM.[100]

HIC as well as reversed-phase chromatography (RP) can be applied to analyze hydrophobicity of different monoclonal antibodies. However, while HIC is non-denaturing for proteins, RP conditions, i.e., elevated temperature and organic solvents as mobile phase, lead to denaturation of proteins. The retention mechanism is based on hydrophobic interactions of the protein with the stationary phase. In general, stationary phase materials are less hydrophobic than common RP stationary phases. Elution in HIC is performed by an inverse gradient meaning that the ionic strength of the mobile phase is decreased during the gradient elution. The lyotropic or Hoffmeister series determines the influence of different salts on the hydrophobic interaction. Anions such as phosphate, sulfate, acetate or chloride promote hydrophobic interactions and protein precipitation in combination with cations such as ammonium, potassium or sodium. Typically, sodium or ammonium sulfate as well as sodium chloride or ammonium acetate are applied as mobile phase in HIC. In comparison to IEX or SEC, high salt concentrations are applied in HIC which depend on the strength according to

the lyotropic series. While weaker salts are applied at concentrations of 3 – 5 M, stronger salts can be effective at 1 – 1.5 M concentration. The addition of organic modifier such as isopropyl alcohol can improve the retention and selectivity, however, applying salt gradient elution is the most effective way for method development.[103]

In addition to IEX, SEC, and HIC, RP and HILIC can be found as biochromatographic modes for protein analysis.[97, 104] However, organic solvents commonly used as mobile phase in RP and HILIC cause denaturation of proteins which limit their application in online coupling with RS. Besides, affinity chromatography (AC) provides an alternative selectivity which is based on a highly specific interaction of the protein with a distinct affinity ligand bound to the stationary phase.[105] However, the affinity to certain ligands is not a universal property of proteins. Thus, the applicability of AC coupled with RS would be limited to specific protein classes, e.g. immunoglobulin G1. Organic buffers used in IEX would be challenging as these compounds have a higher number of bonds, potentially leading to more bands within the Raman spectrum which could obscure protein Raman bands. The same applies to organic anions such as acetate or citrate which might be used in HIC, besides inorganic anions. Inorganic buffers are favorable for coupling IEX or HIC with RS. Therefore, salt gradient elution in IEX would be advantageous over pH gradient elution. Considering the data processing and removal of the mobile phase Raman bands from the analyte spectra, isocratic elution performed in SEC is beneficial in comparison to gradient elution of IEX and HIC. However, gradient elution might yield higher resolution and sharper peak profiles. On the other hand, method development in IEX and HIC is more challenging due to the gradient elution where different salts directly influence the selectivity of the phase system.

1.4 Proteins analyzed within the thesis

1.4.1 Serum albumin

Bovine serum albumin (BSA) and porcine serum albumin (PSA) are globular proteins from different species with molecular weights of approximately 66.4 kDa (BSA)[106] and 67.5 kDa (PSA).[107] Serum albumin maintains oncotic pressure[108] and transports a wide range of endogenous and exogenous molecules (including hormones, vitamins, minerals, and drugs). The various molecules bind to numbers of different binding sites to be transported through the blood stream.[109] It is the most abundant protein in the plasma of mammals.[108] BSA and PSA share a sequence identity of 79.2 % and a sequence similarity of 87.1 %.[110]

BSA and PSA are initially expressed *in vivo* as pre-proalbumin (607 amino acids) containing a signal sequence and an additional propeptide. However, the mature proteins both have a sequence length of 583 amino acids.[108, 111] The three-dimensional structures of BSA and PSA are demonstrated in Figure 1-8.

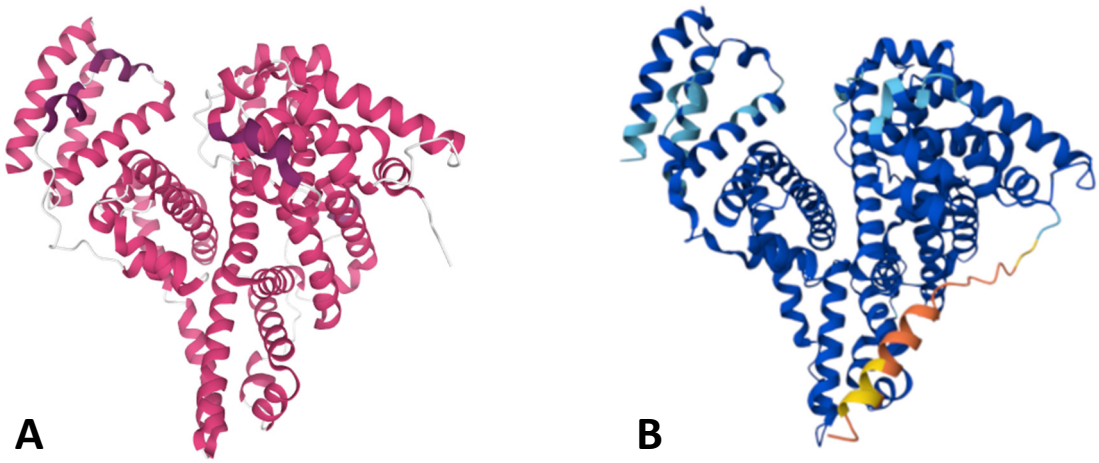

Figure 1-8: Three-dimensional structures of BSA (A) and PSA (B). BSA (PBD-ID: 4F5S) was taken from Bujacz et al.[109, 112] PSA (AF-P08835-F1-v4).[113] was predicted by AlphaFold.[114, 115] Model confidence as per-residue confidence score (pLDDT) and coloring code of the predicted structure (B): very high (pLDDT > 90, dark blue), confident (90 > pLDDT > 70, light blue), low (70 > pLDDT > 50, yellow), very low (pLDDT < 50, orange).

Serum albumin is built from three domains.[109] The secondary structure of BSA consists mainly of α-helices (74 %) in addition to turns.[106]

BSA is used in the production process of different vaccines. Therefore, various vaccines contain residual amounts of BSA which can be found in the prescribing information of the drug products.[116-118]

1.4.2 Hen egg white lysozyme

Hen egg white lysozyme (HEWL) is a globular protein with a molecular weight of 14.3 kDa and a sequence of 129 amino acids.[77, 106] The biological function of HEWL is breaking down bacterial cell walls, thus, providing an antimicrobial activity.[106] The three-dimensional structure of HEWL is depicted in Figure 1-9.

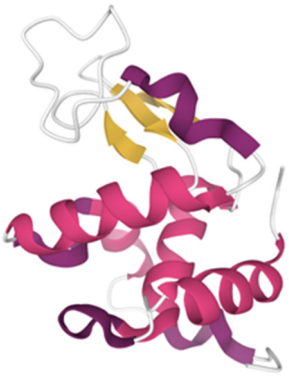

Figure 1-9: Three-dimensional structure of HEWL (PDB-ID: 2EPE) taken from Naresh et al.[119]

HEWL has two domains and four intramolecular disulfide bridges. One domain consists of four α-helices and a 3_{10}-helix whereas the other domain contains a triple-stranded antiparallel β-sheet.[78, 106]

1.4.3 β-lactoglobulin

Bovine β-lactoglobulin (bLG) can be obtained from cow's milk. It has a sequence of 162 amino acids and a molecular weight of 18.4 kDa.[120] BLG forms stable dimers in solution in the pH range between 3.5 and 8.5. BLG enables binding and transport of small hydrophobic molecules such as fatty acids and retinoids. However, its biological function remains still unknown.[121] The conformation of bLG is demonstrated in Figure 1-10.

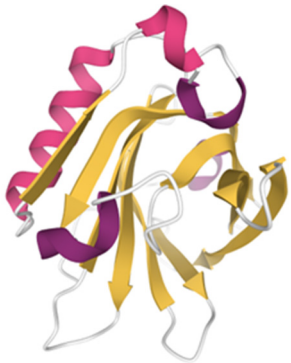

Figure 1-10: Three-dimensional structure of bLG (PDB-ID: 3NPO) taken from Loch et al.[121, 122]

BLG belongs to the family of lipocalins which is a group of proteins with a characteristic β-barrel structure, the so-called calyx. The β-barrel assembles from eight-strands and

is surrounded by flexible loops. The loops are sensitive to pH changes which cause them to reversibly close or open access to the β-barrel core. The inside of the β-barrel is a binding pocket for the hydrophobic molecules. In addition, bLG contains an α-helix and a single β-strand that is organized in a β-α-β motif with one β-strand of the calyx.

The formation of dimers is enabled by the formation of hydrogen bonds between the single β-strands within each monomer. Two intra-molecular disulfide bridges stabilize the tertiary structure of the protein.[121]

1.4.4 Immunoglobulin G

Immunoglobulin G (IgG) antibodies have a molecular weight of approximately 150 kDa. IgG assembles from two identical heavy chains and two identical light chains. Disulfide bonds between both heavy chains and between each heavy and a light chain connect the four individual polypeptide chains.[123] IgG has a Y-shaped conformation with two fragment antigen binding sites (F_{ab}) at the variable regions and the fragment crystallizable (F_c) at the constant regions as demonstrated in Figure 1-11. Antibodies specifically bind to targeted antigens at both their F_{ab} and mediate reactions of the immune system by binding at the F_c to certain receptor molecules of other components of the immune system.[43, 123] Each of the F_{ab} consists of two characteristic β-barrel structures that both arise from two anti-parallel β-sheet structures that are each connected with an intramolecular disulfide bridge. The individual strands of the β-sheets are connected by loops. The F_c assembles from two distinct domains CH2 and CH3 (see Figure 1-11). Additional antiparallel β-sheet structures in combination with less ordered conformation can be observed in Figure 1-11 for that part. Furthermore, the glycosylation sites with the glycans are at the CH2 domain.[93]

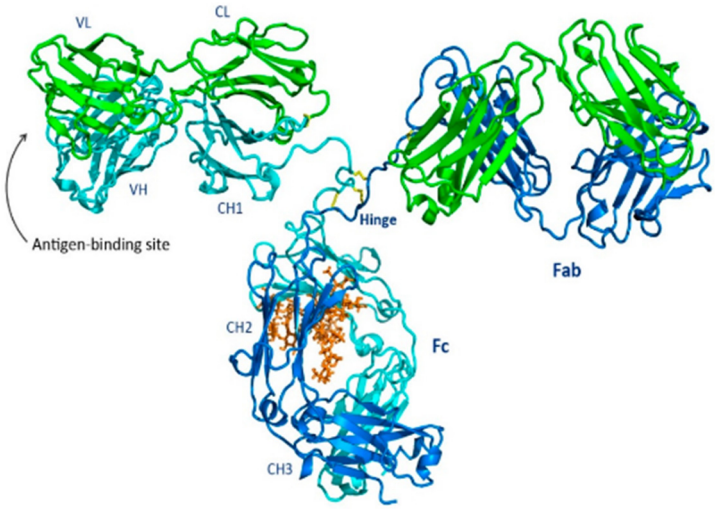

Figure 1-11: Three-dimensional structure of an IgG2 mouse antibody (PDB-ID: 1IGT)[124, 125] taken from Chiu et al.[43] The light chains are green, the heavy chains are cyan and blue, the glycosylation sites are orange and disulfide bonds are yellow.

Rituximab, bevacizumab and daratumumab are monoclonal IgG1 antibodies that are produced by recombinant technology in CHO cell lines.[126-128] Rituximab (RTX) is a

chimeric antibody consisting of human constant regions and murine heavy and light chain variable region sequences. RTX targets the transmembrane antigen CD20 and is indicated for the treatment of non-Hodgkin's lymphoma, chronic lyphocytic leukaemia, rheumatoid arthritis, granulomatosis with plyangiitis and microscopic polyangiitis, and pemphigus vulgaris.[126] Bevacizumab (BVCZ) is a humanized antibody which means that it contains murine complementarity-determining regions and a human framework. BVCZ binds to and inhibits the human vascular endothelial growth factor. BVCZ is approved for the treatment of metastatic colorectal cancer, first-line non-squamous non-small cell lung cancer, recurrent glioblastoma, metastatic renal cell carcinoma, and persistent, recurrent, or metastatic cervical cancer.[127] Daratumumab (DRTM) is a human antibody which is indicated to treat multiple myeloma. DRTM binds to the CD38 antigen.[128] Porcine serum contains IgG of six different subclasses.[129]

1.4.5 Hemoglobin

Hemoglobin (Hb) is responsible for the transport of molecular oxygen in the body. Bovine and porcine Hb have a sequence of 572 and 574 amino acid residues and a molecular weight of approximately 64.7 kDa and 64.8 kDa, respectively.[130, 131] The conformation of Hb is shown in Figure 1-12.

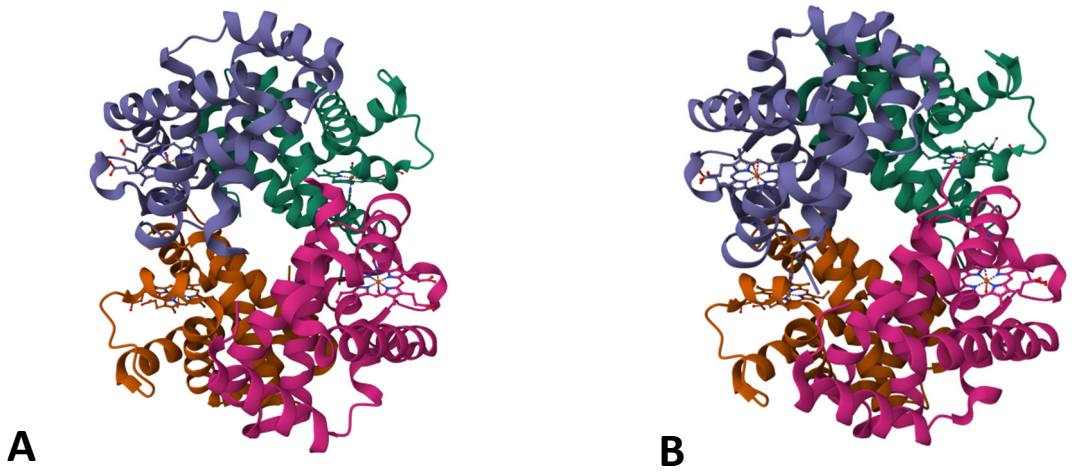

Figure 1-12: Three-dimensional structure of bovine Hb (A, PDB-ID: 2QSS) and porcine Hb (B, PDB-ID: 1QPW) taken from Aranda et al.[131, 132] and Lu et al.,[130, 133] respectively.

Hb is a tetramer which assembles from two α-subunits and two β-subunits. Hb has a ring-shaped conformation with alternating α and β-subunits and a central water cavity. The α-subunits consist of 7 helices, while the β-subunits assemble from 8 helices. Each subunit has a binding pocket formed by two helices where one is covalently bound to the heme prosthetic group. Heme is a complex with a central iron atom coordinated by a porphyrin ring and enables oxygen binding through complex bonding. Allosteric changes in the structure enable binding and release of oxygen at the different tissues.[44]

1.5 Aims and Scope

The online coupling of Raman spectroscopic detection (RS) to liquid chromatography (LC) can be particularly advantageous as RS provides selective structural information on molecules which can be used to identify various analytes. Thus, RS detection could complement concentration-based detectors such as UV or RI by adding structural and conformational insights. In general, RS is highly compatible with aqueously buffered or saline media which provide native conditions for proteins and therefore, particularly suitable for the structural analysis of proteins. Specific information on the higher-order structure can be obtained label-free and non-destructively, in addition to the detection of conformational changes as outlined in chapter 1.3.1. Chapter 1.1.2 highlighted the state-of-the-art in RS detection after chromatographic separation. The chapter revealed that studies mainly focused on pure compounds or artificial mixtures of selected analytes rather than on real samples. Therefore, this thesis should focus on the analysis of proteins in biopharmaceutical or biological samples to outline the possibilities to identify and analyze proteins in complex samples. In addition, the opportunities to characterize biopharmaceutical drug products should be addressed within the thesis.

Thus, the main aim of this thesis is to explore the possibilities and limitations of applying RS detection to LC for investigating proteins and their prosthetic groups in biopharmaceutical or biological samples, thereby addressing various bioanalytical research questions. An overview of the main aspects of the thesis is visually depicted in Figure 1-13.

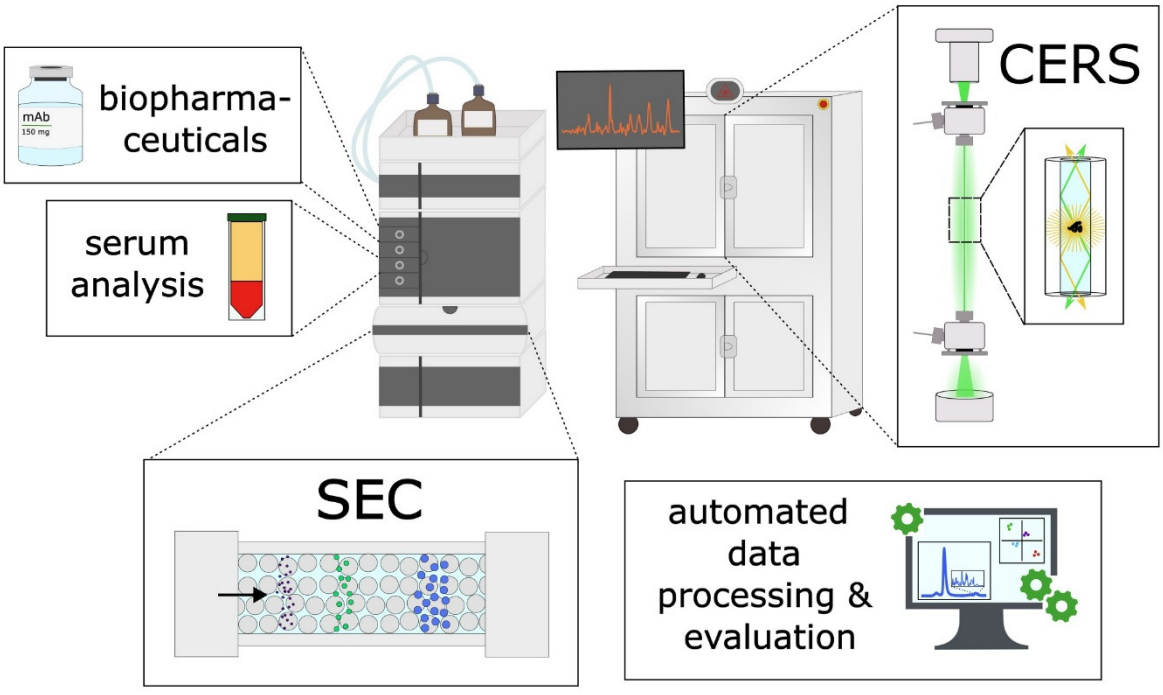

Figure 1-13: Table of contents graphic.

The two analytical instruments, i.e. LC system and RS detector, are in the center of Figure 1-13. In the context of this work, “online coupling” means that the RS detection system is connected to the LC system via a flow path, while simultaneously enabling electronic signal transmission from the LC system to the RS detector. This allows spectra to be recorded in real time, while no additional external control is required during the measurements. The column compartment of the LC system contains the SEC column, which enables the separation of proteins from aggregates and low-molecular weight substances based on the hydrodynamic size of the molecules. SEC was chosen as chromatographic mode due to its importance in the characterization of biopharmaceutical products as outlined in chapter 1.3.1. In addition, the aqueous buffers commonly used in SEC provide native conditions for proteins preserving their conformation and are highly compatible with RS detection due to the relatively weak and broad Raman signal of water. Furthermore, the isocratic elution is beneficial for data processing since it leads to a constant Raman signal of the mobile phase which only changes when compounds elute.

In chapter 2 of the thesis, the detailed set-up of the online coupling, the principle of the LCW detection cell, and a brief overview on the state-of-the-art in online coupling LC and RS are provided. The term capillary-enhanced Raman spectroscopy (CERS), which derives from the effect that the LCW enhances the intensity of the scattered light at the detector, is coined in chapter 2. Furthermore, structural analysis of various well-characterized proteins and a therapeutic protein in a biopharmaceutical product is performed in chapter 2 as illustrated by the drug vial in Figure 1-13. In addition, the detection limit for the functional excipient sucrose was determined to investigate the quantitative capabilities of the detector. Initial considerations regarding complex data processing were described and investigated.

While chapter 2 deals with the establishment of the technique, starting with measurements of model proteins to a more complex sample such as a biopharmaceutical drug, chapter 3 should examine an even more complex sample such as blood serum. Serum is a natural mixture of many different classes of proteins. In Figure 1-13, the analysis of serum is depicted by the Greiner tube with a centrifuged blood sample. Chapter 3 focuses on the identification of different protein classes in hemolyzed serum. In addition, different oxidation and binding states of the heme prosthetic group of hemoglobin were investigated to find an adequate reference for identification of hemoglobin in serum. The hit quality index was established as a parameter for evaluating the similarity and purity of spectra and thus for the objective identification of substances.

Chapters 2 and 3 revealed that the data pre-processing and evaluation of the coupled analysis system are extremely complex due to the multi-dimensionality of the data and require a significant amount of time if executed manually. In addition, a reproducible data pre-processing workflow is essential to reliably recognize and evaluate significant differences between various spectra. Therefore, chapter 4 focuses on the automated data pre-processing and evaluation for the comprehensive analysis of various biopharmaceuticals. Chapter 4 aims to investigate the capabilities of SEC-CERS to

distinguish monoclonal antibodies of the same protein class. In Figure 1-13, this is demonstrated by the monitor showing a chromatogram, a spectrum and a scores diagram of a principal component analysis.

1.6 Referenzen

(1) R.L. McCreery. Introduction and scope. In: *Raman spectroscopy for chemical analysis*, John Wiley & Sons, 2000; pp 1-14.

(2) R.L. McCreery. Magnitude of raman scattering. In: *Raman spectroscopy for chemical analysis*, John Wiley & Sons, 2000; pp 15-33.

(3) *Raman spectroscopy - Theory and practice*; 1st ed.; H.A. Szymanski ed.; Springer New York, 1970. 10.1007/978-1-4684-3027-1:DOI.

(4) W. Kiefer; M. Spiekermann. Special techniques and applications. In: *Infrared and Raman spectroscopy*, VCH Verlagsgesellschaft: Weinheim, 1995; pp 465-517.

(5) C.G. Atkins; K. Buckley; M.W. Blades; R.F.B. Turner, Raman spectroscopy of blood and blood components. *Appl. Spectrosc.* **2017**, *71* (5), 767-793. DOI: 10.1177/0003702816686593.

(6) E.V. Efremov; F. Ariese; C. Gooijer, Achievements in resonance Raman spectroscopy review of a technique with a distinct analytical chemistry potential. *Anal. Chim. Acta* **2008**, *606* (2), 119-134. DOI: 10.1016/j.aca.2007.11.006.

(7) E. Smith; G. Dent. Resonance Raman scattering. In: *Modern Raman spectroscopy - A practical approach*, E. Smith, G. Dent eds.; John Wiley & Sons, 2019; pp 101-117.

(8) C.V. Raman; K.S. Krishnan, A new type of secondary radiation. *Nature* **1928**, *121* (3048), 501-502. DOI: 10.1038/121501c0.

(9) M. D'Orazio; U. Schimpf, On-line detection of mesogenic azoxybenzenes by combined liquid chromatography and Raman spectrometry. *Anal. Chem.* **1981**, *53*, 809-812. DOI: 10.1021/ac00229a016.

(10) K. Iriyama; Y. Ozaki; K. Hibi; T. Ikeda, Raman spectroscopic detection of haemoproteins in the eluate from high-performance liquid chromatography. *J. Chromatogr. A* **1983**, *254*, 285-288. DOI: 10.1016/S0021-9673(01)88345-X.

(11) R. Sheng; F. Ni; T.M. Cotton, Determination of purine bases by reversed-phase high-performance liquid chromatography using real-time surface-enhanced Raman spectroscopy. *Anal. Chem.* **1991**, *63*, 437-442. DOI: 10.1021/ac00005a010.

(12) B.J. Marquardt; P.G. Vahey; R.E. Synovec; L.W. Burgess, A Raman waveguide detector for liquid chromatography. *Anal. Chem.* **1999**, *71* (21), 4808-4814. DOI: 10.1021/ac9907336.

(13) T.D. Nguyen Hong; M. Jouan; N. Quy Dao; M. Bouraly; F. Mantisi, Coupling of high-performance liquid chromatography with Raman spectrometry. *J. Chrom. A* **1996**, *743* (2), 323-327. DOI: 10.1016/0021-9673(96)00303-2.

(14) J. Thissen; M.D. Klassen; P. Constantinidis; M.C. Hacker; J. Breitkreutz; T. Teutenberg; B. Fischer, Online coupling of size exclusion chromatography to capillary enhanced Raman spectroscopy for the analysis of proteins and biopharmaceutical drug products. *Anal. Chem.* **2023**, *95* (48), 17868-17877. DOI: 10.1021/acs.analchem.3c03991.

(15) G.E. Walrafen; J. Stone, Intensification of spontaneous Raman spectra by use of liquid core optical fibers. *Appl. Spectrosc.* **1972**, *26* (6), 585-589. DOI: 10.1366/000370272774351688.

(16) B. Fischer. Entwicklung eines Raman-detektors zur Integration in eine HT-HPLC/IRMS-Kopplung. Heinrich Heine University Düsseldorf, Düsseldorf, 2015. https://docserv.uni-duesseldorf.de/servlets/DocumentServlet?id=33299.

(17) R. Altkorn; M. Duval Malinsky; R.P. van Duyne; I. Koev, Intensity considerations in liquid core optical fiber Raman spectroscopy. *Appl. Spectrosc.* **2001**, *55* (4), 373-381. DOI: 10.1366/0003702011951939.

(18) R. Altkorn; I. Koev; M.J. Pelletier, Raman performance characteristics of Teflon-AF 2400 liquid-core optical-fiber sample cells. *Appl. Spectrosc.* **1999**, *53* (10), 1169-1176. DOI: 10.1366/0003702991945560.

(19) R. Altkorn; I. Koev; R.P. Van Duyne; M. Litorja, Low-loss liquid-core optical fiber for low-refractive-index liquids: Fabrication, characterization, and application in Raman spectroscopy. *Appl. Opt.* **1997**, *36* (34), 8992-8998. DOI: 10.1364/AO.36.008992.

(20) R.J. Dijkstra; A.N. Bader; G.P. Hoornweg; U.A.T. Brinkmann; C. Gooijer, On-line coupling of column liquid chromatography and Raman spectroscopy using a liquid core waveguide. *Anal. Chem.* **1999**, *71*, 4575-4579.

(21) M.N. Polyanskiy, Refractiveindex.Info database of optical constants. *Sci. Data* **2024**, *11* (94). DOI: 10.1038/s41597-023-02898-2.

(22) M.N. Polyanskiy. *Refractive index database*. https://refractiveindex.info (accessed 04 September 2025).

(23) D. Kottke; B.B. Burckhardt; J. Breitkreutz; B. Fischer, Application and validation of a coaxial liquid core waveguide fluorescence detector for the permeation analysis of desmopressin acetate. *Talanta* **2021**, *226*, 122-145. DOI: 10.1016/j.talanta.2021.122145.

(24) M.J. Pelletier; R. Altkorn, Raman sensitivity enhancement for aqueous protein samples using a liquid-core optical-fiber cell. *Anal. Chem.* **2001**, *73*, 1393-1397. DOI: 10.1021/ac001220y.

(25) R.J. Dijkstra; C.J. Slooten; A. Stortelder; J.B. Buijs; F. Ariese; U.A.T. Brinkman; C. Gooijer, Liquid-core waveguide technology for coupling column liquid chromatography and Raman spectroscopy. *J. Chromatogr. A* **2001**, *918* (1), 25-36. DOI: 10.1016/S0021-9673(01)00721-X.

(26) H. Hiramatsu; T. Saito, Vertical flow apparatus for enhancement and efficient collection of Raman signal. *J. Raman Spectrosc.* **2014**, *45* (2), 208-210. DOI: 10.1002/jrs.4437.

(27) Y.H. Lo; H. Hiramatsu, Online liquid chromatography-Raman spectroscopy using the vertical flow method. *Anal. Chem.* **2020**, *92* (21), 14601-14607. DOI: 10.1021/acs.analchem.0c03015.

(28) Y.-S. Chen; H. Hiramatsu, Sugar analysis using hydrophilic liquid chromatography combined with Raman spectroscopy. *Anal. Chem.* **2025**, *97* (25), 12981-12988. DOI: 10.1021/acs.analchem.4c06076.

(29) J.L. Chávez-Servín; A.I. Castellote; M.C. López-Sabater, Analysis of mono- and disaccharides in milk-based formulae by high-performance liquid chromatography with refractive index detection. *J. Chromatogr. A* **2004**, *1043* (2), 211-215. DOI: 10.1016/j.chroma.2004.06.002.

(30) U. Sharma; P. Bhandari; N. Kumar; B. Singh, Simultaneous determination of ten sugars in tinospora cordifolia by ultrasonic assisted extraction and LC-ELSD. *Chromatographia* **2010**, *71* (7), 633-638. DOI: 10.1365/s10337-010-1520-2.

(31) N. Georgelis; K. Fencil; C.M. Richael, Validation of a rapid and sensitive HPLC/MS method for measuring sucrose, fructose and glucose in plant tissues. *Food Chem.* **2018**, *262*, 191-198. DOI: 10.1016/j.foodchem.2018.04.051.

(32) R.J. Dijkstra; C.T. Martha; F. Ariese; U.A.T. Brinkman; C. Gooijer, On-line identification method in column liquid chromatography: UV resonance Raman spectroscopy. *Anal. Chem.* **2001**, *73*, 4977-4982. DOI: 10.1021/ac0103569.

(33) P. Christen; R. Jaussi; R. Benoit. *Biochemie und Molekularbiologie*, 1 ed.; Springer Spektrum Berlin, 2015. DOI: 10.1007/978-3-662-46430-4.

(34) K.A. Dill; S.B. Ozkan; M.S. Shell; T.R. Weikl, The protein folding problem. *Annu. Rev. Biophys.* **2008**, *37*, 289-316. DOI: 10.1146/annurev.biophys.37.092707.153558.

(35) B. Alberts; A. Johnson; J. Lewis; M. Raff; K. Roberts; P. Walter. *Molecular biology of the cell*; 4th ed.; Garland Science, 2002.

(36) T.M. Gupte; M. Ritt; S. Sivaramakrishnan. Chapter seven - ER/K-link – Leveraging a native protein linker to probe dynamic cellular interactions. In: *Methods in enzymology*, M. Merkx ed.; Vol. 647; Academic Press: 2021; pp 173-208.

(37) F. Soleymani; E. Paquet; H. Viktor; W. Michalowski; D. Spinello, Protein-protein interaction prediction with deep learning: A comprehensive review. *Comput. Struct. Biotechnol. J.* **2022**, *20*, 5316-5341. DOI: 10.1016/j.csbj.2022.08.070.

(38) O. Koch; M. Bocola; G. Klebe, Cooperative effects in hydrogen-bonding of protein secondary structure elements: A systematic analysis of crystal data using secbase. *Proteins: Structure, Function, and Bioinformatics* **2005**, *61* (2), 310-317. DOI: 10.1002/prot.20613.

(39) W. Jiskoot; D.J.A. Crommelin. Biophysical and biochemical characteristics of therapeutic proteins. In: *Pharmaceutical biotechnology*, 5th ed.; D.J.A. Crommelin, R.D. Sindelar, B. Meibohm eds.; Springer Nature Switzerland, 2019.

(40) B. Leader; Q.J. Baca; D.E. Golan, Protein therapeutics: A summary and pharmacological classification. *Nat. Rev. Drug Discovery* **2008**, *7* (1), 21-39. DOI: 10.1038/nrd2399.

(41) G. Devitt; K. Howard; A. Mudher; S. Mahajan, Raman spectroscopy: An emerging tool in neurodegenerative disease research and diagnosis. *ACS Chem. Neurosc.* **2018**, *9* (3), 404-420. DOI: 10.1021/acschemneuro.7b00413.

(42) D. Fraser-Pitt; D. O'Neil, Cystic fibrosis – a multiorgan protein misfolding disease. *Future Sci. OA* **2015**, *1* (2). DOI: 10.4155/fso.15.57.

(43) M.L. Chiu; D.R. Goulet; A. Teplyakov; G.L. Gilliland, Antibody structure and function: The basis for engineering therapeutics. *Antibodies* **2019**, *8* (4), 55. DOI: 10.3390/antib8040055.

(44) M.H. Ahmed; M.S. Ghatge; M.K. Safo. Hemoglobin: Structure, function and allostery. In: *Vertebrate and invertebrate respiratory proteins, lipoproteins and other body fluid proteins*, U. Hoeger, J.R. Harris eds.; Springer International Publishing: Cham, 2020; pp 345-382.

(45) R. Aebersold; J.N. Agar; I.J. Amster; M.S. Baker; C.R. Bertozzi; E.S. Boja; C.E. Costello; B.F. Cravatt; C. Fenselau; B.A. Garcia; et al., How many human proteoforms are there? *Nat. Chem. Biol.* **2018**, *14* (3), 206-214. DOI: 10.1038/nchembio.2576.

(46) S.B. Ebrahimi; D. Samanta, Engineering protein-based therapeutics through structural and chemical design. *Nat. Commun.* **2023**, *14* (1), 2411. DOI: 10.1038/s41467-023-38039-x.

(47) C.H. Best; D.A. Scott, The preparation of insulin. *J. Biol. Chem.* **1923**, *57* (3), 709-723. DOI: 10.1016/S0021-9258(18)85482-5.

(48) P.S. Slathia; Sagrika; E. Sharma; I.A. Khan; R.S. Thakur; P. Sharma. Recombinant production of therapeutic proteins. In: *Protein-based therapeutics*, D.B. Singh, T. Tripathi eds.; Springer Nature Singapore, 2023; pp 101-129.

(49) H.A. Parray; S. Shukla; S. Samal; T. Shrivastava; S. Ahmed; C. Sharma; R. Kumar, Hybridoma technology a versatile method for isolation of monoclonal antibodies, its applicability across species, limitations, advancement and future perspectives. *Int. Immunopharmacol.* **2020**, *85*, 106639. DOI: 10.1016/j.intimp.2020.106639.

(50) P.-S. Huang; S.E. Boyken; D. Baker, The coming of age of de novo protein design. *Nature* **2016**, *537* (7620), 320-327. DOI: 10.1038/nature19946.

(51) V. Kumar; A. Barwal; N. Sharma; D.S. Mir; P. Kumar; V. Kumar, Therapeutic proteins: Developments, progress, challenges, and future perspectives. *3 Biotech* **2024**, *14* (4), 112. DOI: 10.1007/s13205-024-03958-z.

(52) W.-P. Alejandra; J.-P. Miriam Irene; G.-S. Fabio Antonio; R.-G.R. Patricia; T.-A. Elizabeth; J.P. Aleman-Aguilar; G.-V. Rebeca, Production of monoclonal antibodies for therapeutic purposes: A review. *Int. Immunopharmacol.* **2023**, *120*, 110376. DOI: 10.1016/j.intimp.2023.110376.

(53) X. Guan; T. Eris; L. Zhang; D. Ren; M.S. Ricci; T. Thiel; C.T. Goudar, A high-resolution multi-attribute method for product characterization, process characterization, and quality control of therapeutic proteins. *Anal. Biochem.* **2022**, *643*, 114575. DOI: 10.1016/j.ab.2022.114575.

(54) W. Wang; S. Singh; D.L. Zeng; K. King; S. Nema, Antibody structure, instability, and formulation. *J. Pharm. Sci.* **2007**, *96* (1), 1-26. DOI: 10.1002/jps.20727.

(55) A.J. Castañeda Ruiz; M.A. Shetab Boushehri; T. Phan; S. Carle; P. Garidel; J. Buske; A. Lamprecht, Alternative excipients for protein stabilization in protein therapeutics: Overcoming the limitations of polysorbates. *Pharmaceutics* **2022**, *14* (12), 2575. DOI: 10.3390/pharmaceutics14122575.

(56) S. Mitragotri; P.A. Burke; R. Langer, Overcoming the challenges in administering biopharmaceuticals: Formulation and delivery strategies. *Nat. Rev. Drug Discovery* **2014**, *13* (9), 655-672. DOI: 10.1038/nrd4363.

(57) S.J. Shire; Z. Shahrokh; J. Liu, Challenges in the development of high protein concentration formulations. *J. Pharm. Sci.* **2004**, *93* (6), 1390-1402. DOI: 10.1002/jps.20079.

(58) D.J.A. Crommelin; A. Hawe; W. Jiskoot. Formulation of biologics including biopharmaceutical considerations. In: *Pharmaceutical biotechnology*, 5th ed.; D.J.A. Crommelin, R.D. Sindelar, B. Meibohm eds.; Springer Nature Switzerland, 2019.

(59) J. Lücke; M. Bädeker; M. Hildinger. *Medizinische Biotechnologie in Deutschland 2025*; Verband Forschender Arzneimittelhersteller (vfa), 2025.

(60) P. Verdin, Top product forecasts for 2025. *Nat. Rev. Drug Discovery* **2025**, *24* (1), 8. DOI: 10.1038/d41573-024-00199-w.

(61) Y. Song; J. Li; Y. Wu, Evolving understanding of autoimmune mechanisms and new therapeutic strategies of autoimmune disorders. *Signal Transduction and Targeted Ther.* **2024**, *9* (1), 263. DOI: 10.1038/s41392-024-01952-8.

(62) S.M. Jung; W.-U. Kim, Targeted immunotherapy for autoimmune disease. *Immune Netw.* **2022**, *22* (1). DOI: 10.4110/in.2022.22.e9.

(63) M. Kędzierska; M. Bańkosz, Role of proteins in oncology: Advances in cancer diagnosis, prognosis, and targeted therapy – A narrative review. *J. Clin. Med.* **2024**, *13* (23), 7131. DOI: 10.3390/jcm13237131.

(64) R. Zaman; R.A. Islam; E.H. Chowdhury, Evolving therapeutic proteins to precisely kill cancer cells. *J. Controlled Release* **2022**, *351*, 779-804. DOI: 10.1016/j.jconrel.2022.09.066.

(65) M.U. Callaghan; R. Sidonio; S.W. Pipe, Novel therapeutics for hemophilia and other bleeding disorders. *Blood* **2018**, *132* (1), 23-30. DOI: 10.1182/blood-2017-09-743385.

(66) J. Cummings; A.M.L. Osse; D. Cammann; J. Powell; J. Chen, Anti-amyloid monoclonal antibodies for the treatment of Alzheimer's disease. *BioDrugs* **2024**, *38* (1), 5-22. DOI: 10.1007/s40259-023-00633-2.

(67) S. Subramaniam; J.W. Saville; F. Feng; L. Freiburger, Therapeutic antibodies for infectious diseases: Recent past, present, and future. *Biochemistry* **2025**, *64* (16), 3487-3494. DOI: 10.1021/acs.biochem.5c00192.

(68) H. Keen; J.C. Pickup; R.W. Bilous; A. Glynne; G.C. Viberti; R.J. Jarrett; R. Marsden, Human insulin produced by recombinant DNA technology: Safety and hypoglycaemic potency in healthy men. *The Lancet* **1980**, *316* (8191), 398-401. DOI: 10.1016/S0140-6736(80)90443-2.

(69) J.L. Rosado; N.W. Solomons; R. Lisker; H. Bourges; G. Anrubio; A. García; R. Perez-Briceño; E. Aizupuru, Enzyme replacement therapy for primary adult lactase deficiency: Effective reduction of lactose malabsorption and milk intolerance by direct addition of β-galactosidase to milk at mealtime. *Gastroenterology* **1984**, *87* (5), 1072-1082. DOI: 10.1016/S0016-5085(84)80067-0.

(70) S. Paul; M.F. Konig; D.M. Pardoll; C. Bettegowda; N. Papadopoulos; K.M. Wright; S.B. Gabelli; M. Ho; A. van Elsas; S. Zhou, Cancer therapy with antibodies. *Nat. Rev. Cancer* **2024**, *24* (6), 399-426. DOI: 10.1038/s41568-024-00690-x.

(71) Z. Fu; S. Li; S. Han; C. Shi; Y. Zhang, Antibody drug conjugate: The "biological missile" for targeted cancer therapy. *Signal Transduction and Targeted Ther.* **2022**, *7* (1), 93. DOI: 10.1038/s41392-022-00947-7.

(72) D.M. Granoff; A. Chacko; K.R. Lottenbach; K.E. Sheetz, Immunogenicity of haemophilus influenzae type b polysaccharide-outer membrane protein conjugate vaccine in patients who acquired haemophilus disease despite previous vaccination with type b polysaccharide vaccine. *J. Pediatr.* **1989**, *114* (6), 925-933. DOI: 10.1016/S0022-3476(89)80432-9.

(73) M. Kheirvari; H. Liu; E. Tumban, Virus-like particle vaccines and platforms for vaccine development. *Viruses* **2023**, *15* (5), 1109. DOI: 10.3390/v15051109.

(74) C. Duranti; A. Arcangeli, Ion channel targeting with antibodies and antibody fragments for cancer diagnosis. *Antibodies* **2019**, *8* (2), 33. DOI: 10.3390/antib8020033.

(75) N.C. Maiti; M.M. Apetri; M.G. Zagorski; P.R. Carey; V.E. Anderson, Raman spectroscopic characterization of secondary structure in natively unfolded proteins: α-synuclein. *J. Am. Chem. Soc.* **2004**, *126* (8), 2399-2408. DOI: 10.1021/ja0356176.

(76) G. Devitt; W. Rice; A. Crisford; I. Nandhakumar; A. Mudher; S. Mahajan, Conformational evolution of molecular signatures during amyloidogenic protein aggregation. *ACS Chem. Neurosc.* **2019**, *10* (11), 4593-4611. DOI: 10.1021/acschemneuro.9b00451.

(77) L. Xing; W. Fan; N. Chen; M. Li; X. Zhou; S. Liu, Amyloid formation kinetics of hen egg white lysozyme under heat and acidic conditions revealed by Raman spectroscopy. *J. Raman Spectrosc.* **2019**, *50* (5), 629-640. DOI: 10.1002/jrs.5567.

(78) S. Dolui; A. Mondal; A. Roy; U. Pal; S. Das; A. Saha; N.C. Maiti, Order, disorder, and reorder state of lysozyme: Aggregation mechanism by Raman spectroscopy. *J. Phys. Chem. B* **2020**, *124* (1), 50-60. DOI: 10.1021/acs.jpcb.9b09139.

(79) S. Dolui; A. Roy; U. Pal; S. Kundu; E. Pandit; B. N Ratha; R. Pariary; A. Saha; A. Bhunia; N.C. Maiti, Raman spectroscopic insights of phase-separated insulin aggregates. *ACS Phys. Chem. Au* **2024**, *4* (3), 268-280. DOI: 10.1021/acsphyschemau.3c00065.

(80) N.S.M. Nor Ihsan; S.F. Abdul Sani; L.M. Looi; D. Pathmanathan; P.L. Cheah; S.F. Chiew; D.A. Bradley, Raman spectroscopic signatures of amyloid fibrils: Insights into structural and biochemical changes in human tissues. *Biophysical Chem.* **2025**, *325*, 107480. DOI: 10.1016/j.bpc.2025.107480.

(81) B. Lochocki; T.H.J. Morrema; F. Ariese; J.J.M. Hoozemans; J.F. de Boer, The search for a unique Raman signature of amyloid-beta plaques in human brain tissue from Alzheimer's disease patients. *Analyst* **2020**, *145* (5), 1724-1736. DOI: 10.1039/C9AN02087J.

(82) J.H. Kim; C. Zhang; C.J. Sperati; S.M. Bagnasco; I. Barman, Non-perturbative identification and subtyping of amyloidosis in human kidney tissue with Raman spectroscopy and machine learning. *Biosensors* **2023**, *13* (4), 466. DOI: 10.3390/bios13040466.

(83) J. Thissen. Raman-spektroskopische Identifizierung von Proteinen und stressinduzierten Proteinaggregaten in Lösung. Master Thesis, Hochschule Niederrhein, Krefeld, 2021.

(84) I. Ettah; L. Ashton, Engaging with Raman spectroscopy to investigate antibody aggregation. *Antibodies* **2018**, *7* (3), 24. DOI: 10.3390/antib7030024.

(85) A. Rygula; K. Majzner; K.M. Marzec; A. Kaczor; M. Pilarczyk; M. Baranska, Raman spectroscopy of proteins: A review. *J. Raman Spectrosc.* **2013**, *44* (8), 1061-1076. DOI: 10.1002/jrs.4335.

(86) Z.Q. Wen, Raman spectroscopy of protein pharmaceuticals. *J. Pharm. Sci.* **2007**, *96* (11), 2861-2878. DOI: 10.1002/jps.20895.

(87) N. Kuhar; S. Sil; S. Umapathy, Potential of Raman spectroscopic techniques to study proteins. *Spectrochim. Acta, Part A* **2021**, *258*, 119712. DOI: 10.1016/j.saa.2021.119712.

(88) H. Takeuchi, Raman structural markers of tryptophan and histidine side chains in proteins. *Biopolymers* **2003**, *72* (5), 305-317. DOI: 10.1002/bip.10440.

(89) C.J. Robinson; C. Jones, Quality control and analytical techniques for biopharmaceuticals. *Bioanalysis* **2011**, *3* (1), 81-95. DOI: 10.4155/bio.10.161.

(90) A. Sadat; I.J. Joye, Peak fitting applied to fourier transform infrared and Raman spectroscopic analysis of proteins. *Appl. Sci.* **2020**, *10* (17), 5918. DOI: 10.3390/app10175918.

(91) J. Peters; C. Jin; A. Luczak; B. Lyons; R. Kalyanaraman, Machine learning enabled protein secondary structure characterization using drop-coating deposition Raman spectroscopy. *J. Pharm. Biomed. Anal.* **2025**, *259*, 116762. DOI: 10.1016/j.jpba.2025.116762.

(92) M.K. Shukla; P. Wilkes; N. Bargary; K. Meagher; D. Khamar; D. Bailey; S.P. Hudson, Identification of monoclonal antibody drug substances using non-destructive Raman spectroscopy. *Spectrochim. Acta, Part A* **2023**, *299*, 122872. DOI: 10.1016/j.saa.2023.122872.

(93) L. Fontana; C. Anderson; R. Bogner; M. Pikal, Evaluation of a Raman chemometric method for detecting protein structural conformational changes in solution. *J. Pharm. Sci.* **2023**, *112* (2), 573-586. DOI: 10.1016/j.xphs.2022.09.006.

(94) J. De Meutter; E. Goormaghtigh, Protein structural denaturation evaluated by MCR-ALS of protein microarray FTIR spectra. *Anal. Chem.* **2021**, *93* (40), 13441-13449. DOI: 10.1021/acs.analchem.1c01416.

(95) ICH Q6B, Specifications: Test procedures and acceptance criteria for biotechnological/biological products. *ICH Harmonised Tripartite Guideline* **1999**, *CPMP/ICH/365/96*.

(96) ICH Q5C, Quality of biotechnological products: Stability testing of biotechnological/biological products. *ICH Harmonised Tripartite Guideline* **1995**, *CPMP/ICH/138/95*.

(97) K. Sandra; I. Vandenheede; P. Sandra, Modern chromatographic and mass spectrometric techniques for protein biopharmaceutical characterization. *J. Chromatogr. A* **2014**, *1335*, 81-103. DOI: 10.1016/j.chroma.2013.11.057.

(98) M. ImioŁek; S. Fekete; S. Rudaz; D. Guillarme, Ion exchange chromatography of biotherapeutics: Fundamental principles and advanced approaches. *J. Chromatogr. A* **2025**, *1742*, 465672. DOI: 10.1016/j.chroma.2025.465672.

(99) S. Fekete; A. Beck; J.-L. Veuthey; D. Guillarme, Ion-exchange chromatography for the characterization of biopharmaceuticals. *J. Pharm. Biomed. Anal.* **2015**, *113*, 43-55. DOI: 10.1016/j.jpba.2015.02.037.

(100) S. Fekete; A. Beck; J.L. Veuthey; D. Guillarme, Theory and practice of size exclusion chromatography for the analysis of protein aggregates. *J. Pharm. Biomed. Anal.* **2014**, *101*, 161-173. DOI: 10.1016/j.jpba.2014.04.011.

(101) A. Koulov. Protein stability and characterization. In: *Pharmaceutical biotechnology*, 5th ed.; D.J.A. Crommelin, R.D. Sindelar, B. Meibohm eds.; Springer Nature Switzerland, 2019.

(102) P. Hong; S. Koza; E.S. Bouvier, Size-exclusion chromatography for the analysis of protein biotherapeutics and their aggregates. *J. Liq. Chromatogr. Relat. Technol.* **2012**, *35* (20), 2923-2950. DOI: 10.1080/10826076.2012.743724.

(103) S. Fekete; J.-L. Veuthey; A. Beck; D. Guillarme, Hydrophobic interaction chromatography for the characterization of monoclonal antibodies and related products. *J. Pharm. Biomed. Anal.* **2016**, *130*, 3-18. DOI: 10.1016/j.jpba.2016.04.004.

(104) S. Tengattini; G. Massolini; F. Rinaldi; E. Calleri; C. Temporini, Hydrophilic interaction liquid chromatography (HILIC) for the analysis of intact proteins and glycoproteins. *TrAC, Trends Anal. Chem.* **2024**, *174*, 117702. DOI: 10.1016/j.trac.2024.117702.

(105) E.L. Rodriguez; S. Poddar; S. Iftekhar; K. Suh; A.G. Woolfork; S. Ovbude; A. Pekarek; M. Walters; S. Lott; D.S. Hage, Affinity chromatography: A review of trends and developments over the past 50 years. *J. Chromatogr. B* **2020**, *1157*, 122332. DOI: 10.1016/j.jchromb.2020.122332.

(106) S. Lee; M.C. Choi; K. Al Adem; S. Lukman; T.-Y. Kim, Aggregation and cellular toxicity of pathogenic or non-pathogenic proteins. *Sci. Rep.* **2020**, *10* (1), 5120. DOI: 10.1038/s41598-020-62062-3.

(107) R.N.K. Carlsson; B.I. Ingvarsson; W.K. Börje, Isolation and characterization of albumin from porcine serum, colostrum and urine. *Int. J. Biochem.* **1977**, *8* (4), 285-294. DOI: 10.1016/0020-711X(77)90134-3.

(108) K.A. Majorek; P.J. Porebski; A. Dayal; M.D. Zimmerman; K. Jablonska; A.J. Stewart; M. Chruszcz; W. Minor, Structural and immunologic characterization of bovine, horse, and rabbit serum albumins. *Mol. Immunol.* **2012**, *52* (3-4), 174-182. DOI: 10.1016/j.molimm.2012.05.011.

(109) A. Bujacz, Structures of bovine, equine and leporine serum albumin. *Acta Crystallogr. D Biol. Crystallogr.* **2012**, *68* (10), 1278-1289. DOI: 10.1107/S0907444912027047.

(110) M. Chruszcz; K. Mikolajczak; N. Mank; K.A. Majorek; P.J. Porebski; W. Minor, Serum albumins – unusual allergens. *Biochim. Biophys. Acta, Gen. Subj.* **2013**, *1830* (12), 5375-5381. DOI: 10.1016/j.bbagen.2013.06.016.

(111) J. Weinstock; G.S. Baldwin, Nucleotide sequence of porcine liver albumin. *Nucleic Acids Res.* **1988**, *16* (18), 9045. DOI: 10.1093/nar/16.18.9045.

(112) A. Bujacz; G. Bujacz, Crystal structure of bovine serum albumin. PDB ID: 4F5S. DOI: 10.2210/pdb4F5S/pdb.

(113) DeepMind. *Alphafold protein structure database*. UniProt ID: P08835, Version: AF-P08835-F1-v4. https://www.alphafold.ebi.ac.uk/entry/P08835 (accessed 04 July 2025).

(114) J. Jumper; R. Evans; A. Pritzel; T. Green; M. Figurnov; O. Ronneberger; K. Tunyasuvunakool; R. Bates; A. Žídek; A. Potapenko; et al., Highly accurate protein structure prediction with Alphafold. *Nature* **2021**, *596* (7873), 583-589. DOI: 10.1038/s41586-021-03819-2.

(115) M. Varadi; D. Bertoni; P. Magana; U. Paramval; I. Pidruchna; M. Radhakrishnan; M. Tsenkov; S. Nair; M. Mirdita; J. Yeo; et al., Alphafold protein structure database in 2024: Providing structure coverage for over 214 million protein sequences. *Nucleic Acids Res.* **2023**, *52* (D1), D368-D375. DOI: 10.1093/nar/gkad1011.

(116) Sanofi. *Fachinformation: Repevax*. 2021. https://impfen.sanofi.de/dam/jcr:ad51b5cf-8feb-4a6d-a7a0-b441dc1b2065/DE_SPC_Repevax.pdf (accessed 04 July 2025).

(117) MSP Vaccine Company. *Highlights of prescribing information: Vaxelis*. Food and Drug Administration, 2020. https://www.fda.gov/media/119465/download (accessed 04 July 2025).

(118) GlaxoSmithKline. *Highlights of prescribing information: Priorix*. Food and Drug Administration, 2022. https://www.fda.gov/media/158941/download (accessed 04 July 2025).

(119) M.D. Naresh, Subramanian, V., Jaimohan, S.M., Rajaram, A., Arumugam, V., Usha, R., Mandal, A.B., Crystal structure analysis of hen egg white lysozyme grown by capillary method. PDB ID: 2EPE. DOI: 10.2210/pdb2EPE/pdb.

(120) H.C. Liu; W.L. Chen; S.J.T. Mao, Antioxidant nature of bovine milk β-lactoglobulin. *J. Dairy Sci.* **2007**, *90* (2), 547-555. DOI: 10.3168/jds.S0022-0302(07)71538-2.

(121) J. Loch; A. Polit; A. Górecki; P. Bonarek; K. Kurpiewska; M. Dziedzicka-Wasylewska; K. Lewiński, Two modes of fatty acid binding to bovine β-lactoglobulin – crystallographic and spectroscopic studies. *J. Mol. Recognit.* **2011**, *24* (2), 341-349. DOI: 10.1002/jmr.1084.

(122) J.I. Loch; K. Lewinski, Two modes of fatty acid binding to bovine beta-lactoglobulin-crystallographic and spectroscopic studies. PDB ID: 3NPO. DOI: 10.2210/pdb3NPO/pdb.

(123) C.A.J. Janeway; P. Travers; M. Walport; M.J. Shlomchik. The structure of a typical antibody molecule. In: *Immunobiology: The immune system in health and disease*, 5th ed.; Garland Science: New York, 2001.

(124) L.J. Harris; S.B. Larson; K.W. Hasel; A. McPherson, Refined structure of an intact IgG2a monoclonal antibody. *Biochemistry* **1997**, *36* (7), 1581-1597. DOI: 10.1021/bi962514+.

(125) L.J. Harris; S.B. Larson; K.W. Hasel; A. McPherson, Structure of immunoglobulin. PDB ID: 1IGT. DOI: 10.2210/pdb1IGT/pdb.

(126) Sandoz. *Annex I – Summary of product characteristics*. European Medicines Agency, https://www.ema.europa.eu/en/documents/product-information/rixathon-epar-product-information_en.pdf (accessed 15 May 2025).

(127) Genentech. *Avastin: Highlights of prescribing information.* Food and Drug Administration, https://www.accessdata.fda.gov/drugsatfda_docs/label/2022/125085s340lbl.pdf (accessed 15 May 2025).

(128) Janssen. *Darzalex: Highlights of prescribing information*. Food and Drug Administration, https://www.janssenlabels.com/package-insert/product-monograph/prescribing-information/DARZALEX-pi.pdf (accessed 26 July 2024).

(129) J.E. Butler; N. Wertz; N. Deschacht; I. Kacskovics, Porcine IgG: Structure, genetics, and evolution. *Immunogenetics* **2009**, *61* (3), 209-230. DOI: 10.1007/s00251-008-0336-9.

(130) T.H. Lu; K. Panneerselvam; Y.C. Liaw; P. Kan; C.J. Lee, Structure determination of porcine haemoglobin. PDB ID: 1QPW. DOI: 10.2210/pdb1QPW/pdb.

(131) R. Aranda; H. Cai; C.E. Worley; E.J. Levin; R. Li; J.S. Olson; G.N. Phillips; M.P. Richards, Structural analysis of fish versus mammalian hemoglobins: Effect of the heme pocket environment on autooxidation and hemin loss. PDB ID: 2QSS. DOI: 10.2210/pdb2QSS/pdb.

(132) R. Aranda IV; H. Cai; C.E. Worley; E.J. Levin; R. Li; J.S. Olson; G.N. Phillips Jr; M.P. Richards, Structural analysis of fish versus mammalian hemoglobins: Effect of the heme pocket environment on autooxidation and hemin loss. *Proteins: Structure, Function, and Bioinformatics* **2009**, *75* (1), 217-230. DOI: 10.1002/prot.22236.

(133) T.-H. Lu; K. Panneerselvam; Y.-C. Liaw; P. Kan; C.-J. Lee, Structure determination of porcine haemoglobin. *Acta Crystallogr. D Biol. Crystallogr.* **2000**, *56* (3), 304-312. DOI: 10.1107/S0907444900000093.

2 Analysis of proteins and biopharmaceutical drug products

Pretext

In this chapter, a brief literature review of Raman spectroscopic detection coupled with liquid chromatography is provided in order to outline strategies to overcome the low sensitivity of Raman spectroscopic detection and to highlight the novelty of the approach of coupling SEC-CERS. The basic principle of capillary-enhanced Raman spectroscopy (CERS) by applying an LCW for Raman scattering signal enhancement is described as well as the detailed set-up of the analytical instrument. The continuous acquisition of scans without signal averaging and the concentration gradient of the chromatographic elution profile introduced new challenges for CERS data pre-processing in comparison to conventional Raman spectroscopy. These challenges were addressed and evaluated to improve the signal-to-noise ratios in the Raman spectra. SEC-CERS was applied to elucidate and differentiate the higher-order structures of well characterized proteins such as bovine serum albumin, hen egg white lysozyme, and β-lactoglobulin and of the monoclonal antibody rituximab in a biopharmaceutical product. In addition, the functional excipient sucrose in the biopharmaceutical product Zirabev was quantified by CERS to investigate sensitivity and precision of SEC-CERS.

Evaluation of authorship

author	idea [%]	concept [%]	experimental [%]	evaluation [%]	manuscript [%]
Jana Thissen	0	65	100	90	83
Martin D. Klassen	35	10	0	5	4
Philipp Constantinidis	0	3	0	0	2
Michael C. Hacker	0	5	0	0	2
Jörg Breitkreutz	15	5	0	0	2
Thorsten Teutenberg	15	7	0	0	3
Björn Fischer	35	10	0	5	4

Author contributions

Jana Thissen: Conceptualization, Investigation, Data evaluation and Visualization, Writing - Original Draft; Martin D. Klassen: Idea, Conceptualization, Writing - Review & Editing, Supervision, Funding acquisition, Philipp Constantinidis: Conceptualization, Writing - Review & Editing; Michael C. Hacker: Writing - Review & Editing, Supervision; Jörg Breitkreutz: Writing - Review & Editing, Supervision; Thorsten Teutenberg: Idea, Conceptualization, Writing - Review & Editing, Supervision, Funding acquisition; Björn Fischer: Idea, Conceptualization, Writing - Review & Editing, Supervision, Funding acquisition.

The first author JTh was responsible for the conceptualization of the study, executed all experiments, developed a concept for data evaluation, and wrote a first draft of the manuscript. The idea of analyzing proteins and biopharmaceutical products was related to the funding acquisition which was done by MK, TT, BF and JB. All authors were involved in the conceptualization of the study. MK and BF contributed to the development of the data evaluation workflow. MK, PC, MH, JB, TT, and BF reviewed and edited the manuscript.

Online coupling of size exclusion chromatography to capillary enhanced Raman spectroscopy for the analysis of proteins and biopharmaceutical drug products

Jana Thissen[1,2], Martin D. Klassen[1], Philipp Constantinidis[1], Michael C. Hacker[2], Jörg Breitkreutz[2], Thorsten Teutenberg[1,*], and Björn Fischer[2]

[1] Institut für Umwelt & Energie, Technik & Analytik e.V. (IUTA), Duisburg, Germany

[2] Heinrich Heine University Düsseldorf, Faculty of Mathematics and Natural Sciences, Institute of Pharmaceutics and Biopharmaceutics, Düsseldorf, Germany

Anal. Chem. **2023**, *95* (48), 17868 – 17877, DOI: 10.1021/acs.analchem.3c03991.

Abstract

The online coupling of size exclusion chromatography (SEC) to capillary enhanced Raman spectroscopy (CERS) based on a liquid core waveguide (LCW) flow cell was applied for the first time to assess the higher-order structure of different proteins. This setup allows to record Raman spectra of the monomeric protein within complex mixtures, since SEC enables the separation of the monomeric protein from matrix components such as excipients of a biopharmaceutical product and higher molecular weight species (e.g. aggregates). The acquired Raman spectra were used for structural elucidation of well characterized proteins such as bovine serum albumin, hen egg white lysozyme, β-lactoglobulin and of the monoclonal antibody rituximab in a medicinal product. Additionally, the CERS detection of the disaccharide sucrose, which is used as a stabilizing excipient, was quantified to achieve a limit of detection (LOD) of 120 µg and a limit of quantification (LOQ) of 363 µg injected on the column.

Subjects

Carbohydrates · Lasers · Peptides and Proteins · Raman spectroscopy · Size Exclusion Chromatography

3 Identification of protein classes in hemolyzed blood serum

Pretext

In this chapter, the online coupling of SEC-DAD-CERS is applied to identify different protein classes in a highly complex mixture of proteins such as hemolyzed serum. A calculated hit quality index was introduced and discussed to objectively evaluate the similarity and purity of sample spectra in comparison to reference spectra. In addition, different oxidation and binding states of the heme prosthetic group of hemoglobin were investigated in detail.

Evaluation of authorship

author	idea [%]	concept [%]	experimental [%]	evaluation [%]	manuscript [%]
Jana Thissen	50	65	100	96	85
Martin D. Klassen	25	12	0	2	4
Michael C. Hacker	5	5	0	0	2
Jörg Breitkreutz	5	5	0	0	2
Thorsten Teutenberg	5	5	0	0	3
Björn Fischer	10	8	0	2	4

Author contributions

Jana Thissen: Conceptualization, Investigation, Data evaluation and Visualization, Writing - Original Draft; Martin D. Klassen: Conceptualization, Writing - Review & Editing, Supervision, Funding acquisition; Michael C. Hacker: Writing - Review & Editing, Supervision; Jörg Breitkreutz: Writing - Review & Editing, Supervision; Thorsten Teutenberg: Conceptualization, Writing - Review & Editing, Supervision, Funding acquisition; Björn Fischer: Conceptualization, Writing - Review & Editing, Supervision; All authors have read and agreed to the published version of the manuscript.

The first author JTh was responsible for the conceptualization of the study, executed all experiments, developed a concept for data evaluation, and wrote a first draft of the manuscript. All authors contributed to the idea of analyzing serum by SEC-DAD-CERS. MK and BF contributed to the development of the data evaluation workflow. MK, MH, JB, TT and BF contributed to the conceptualization of the study and reviewed and edited the manuscript.

Online coupling of size exclusion chromatography to capillary enhanced Raman spectroscopy for the identification of protein classes in hemolyzed blood serum

Jana Thissen[1,2], Martin D. Klassen[1], Michael C. Hacker[2], Jörg Breitkreutz[2], Thorsten Teutenberg[1,*], and Björn Fischer[2]

[1] Institut für Umwelt & Energie, Technik & Analytik e.V. (IUTA), Duisburg, Germany

[2] Heinrich Heine University Düsseldorf, Faculty of Mathematics and Natural Sciences, Institute of Pharmaceutics and Biopharmaceutics, Düsseldorf, Germany

Anal. Bioanal. Chem. **2025**, *417* (2), 335 – 344, DOI: 10.1007/s00216-024-05649-3.

Abstract

The analysis of serum for biomarkers is a standard method in clinical diagnosis and health assessment. The application of Raman spectroscopy to probe biomarkers in serum is increasingly investigated due to its time- and cost-efficiency. However, time-consuming sample preparation is often required to analyze the serum samples. Additionally, hemolyzed samples are commonly discarded due to interferences in the measurements. This study focuses on the application of the online coupling of size exclusion chromatography (SEC) to diode-array-detector (DAD) and capillary enhanced Raman spectroscopy (CERS) for direct analysis of hemolyzed serum samples. We demonstrate that different protein classes such as serum albumin and immunoglobulin G (IgG) can be identified in hemolyzed serum according to a calculated hit quality index (HQI). Additionally, different oxidation and binding states of the heme prosthetic group are investigated at 532 nm excitation. The online coupling of SEC-DAD-CERS enables the detailed characterization of blood serum proteins, including the differentiation of IgG, serum albumin, and hemoglobin.

Keywords

Size exclusion chromatography · Raman spectroscopy · Protein structural analysis · Serum analysis

4 Comprehensive analysis of various biopharmaceutical products

Pretext

This chapter focuses on the automated data-processing and comprehensive analysis of various biopharmaceutical products analyzed by SEC-CERS. A detailed explanation of the pre-processing steps is provided giving a deeper understanding of the requirements for processing SEC-CERS data. The opportunities of different data-analysis tools such as a hit quality index or a principal component analysis are investigated to address the challenge of objectively differentiating biopharmaceutical products according to their CERS spectra. In addition, the quantification of various compounds based on their Raman spectra is explored by applying multivariate curve resolution – alternating least squares.

Evaluation of authorship

author	idea [%]	concept [%]	experimental [%]	evaluation [%]	manuscript [%]
Jana Thissen	50	60	100	30	75
Martin D. Klassen	0	0	0	0	2
Björn Fischer	0	0	0	0	2
Michael C. Hacker	0	0	0	0	2
Jörg Breitkreutz	0	0	0	0	2
Thorsten Teutenberg	0	0	0	0	2
J. Ricardo Cunha	50	40	0	70	15

Author contributions

Jana Thissen: Conceptualization, Formal analysis, Investigation, Data evaluation and Visualization, Writing - Original Draft; Martin D. Klassen: Writing - Review & Editing, Supervision, Funding acquisition; Björn Fischer: Writing - Review & Editing, Supervision; Thorsten Teutenberg: Writing - Review & Editing, Supervision, Funding acquisition; Björn Fischer: Writing - Review & Editing, Supervision; Michael C. Hacker: Writing - Review & Editing, Supervision; Jörg Breitkreutz: Writing - Review & Editing, Supervision; J. Ricardo Cunha: Conceptualization, Formal analysis, Software Development, Data evaluation and Visualization, Writing - Original Draft, Funding acquisition.

The idea of an automated data processing workflow and the comprehensive analysis of biopharmaceutical products was developed by JTh and RC. The first author JTh and the last author RC contributed mainly to the conceptualization of the study. JTh executed all experiments, contributed to the development of the automated workflow, refined and adjusted parameters of the data processing and evaluation, and wrote most of the first draft of the manuscript. RC developed the software for automated data processing, created workflows for data evaluation, wrote parts of the first draft of the manuscript and created the figures shown in the manuscript. MK, BF, TT, MH and JB reviewed and edited the manuscript.

StreamFind: data processing workflows for qualification and quantification of biopharmaceutical drug products analyzed by size exclusion chromatography coupled to capillary-enhanced Raman spectroscopy

Jana Thissen[1,2], Martin D. Klassen[1], Björn Fischer[2], Michael C. Hacker[2], Jörg Breitkreutz[2], Thorsten Teutenberg[1], and J. Ricardo Cunha[1,*]

[1] Institut für Umwelt & Energie, Technik & Analytik e.V. (IUTA), Duisburg, Germany

[2] Heinrich Heine University Düsseldorf, Faculty of Mathematics and Natural Sciences, Institute of Pharmaceutics and Biopharmaceutics, Düsseldorf, Germany

Anal. Bioanal. Chem. **2025**, *417* (19), 4469 – 4480,
DOI: 10.1007/s00216-025-05964-3.

Abstract

Innovative hyphenated technologies, such as size exclusion chromatography coupled with capillary-enhanced Raman spectroscopy (SEC-CERS), enable more comprehensive analyses of biopharmaceutical drug products. However, specialized software for processing and analyzing data from these advanced techniques is often lacking. This study introduces the R package StreamFind, which is designed to help users seamlessly process both chromatographic and Raman spectroscopic data within an integrated workflow. We detail the implementation and structure of StreamFind and demonstrate its ability in the in-depth analysis of biopharmaceutical products. The study shows its capability to differentiate monoclonal antibodies and entire biopharmaceutical formulations and to quantify various components based on their Raman spectra. Principal component analysis (PCA) identified significant differences among the biopharmaceutical products analyzed, while multivariate curve resolution-alternating least squares (MCR-ALS) proved to be an effective method for quantifying different components within these products. The StreamFind platform is designed to be extensible, to facilitate contributions from new users and to support the future integration of additional algorithms to process different types of complex analytical data.

Keywords

StreamFind · Open-source software · Liquid chromatography · Raman spectroscopy · Biopharmaceuticals

5 Conclusion and Outlook

The present thesis significantly contributed to the field of Raman spectroscopic detection for liquid chromatography by demonstrating the high applicability of online coupled size exclusion chromatography to capillary-enhanced Raman spectroscopy (SEC-CERS) for the analysis of various proteins and components in biopharmaceutical products. In comparison to most of the recent studies on Raman spectroscopic detection for liquid chromatography, SEC-CERS could successfully be applied to complex samples such as serum or biopharmaceutical products and address practical use cases such as the assessment of the higher-order structure in biopharmaceutical characterization or the analysis of biomarkers in hemolyzed serum which highlight the novelty and scientific importance of the present thesis.

Initially, structural elucidation of the structurally well-characterized proteins bovine serum albumin, hen egg white lysozyme, and β-lactoglobulin and the monoclonal antibody rituximab in the biopharmaceutical product Rixathon was performed which outlined the capability of SEC-CERS to differentiate various proteins based on visual evaluation and band assignment of their structure. Rituximab as well as the functional excipient sucrose could be analyzed effectively without sample preparation in common concentration range of the dosage form. Furthermore, the determination of the higher-order structure of therapeutic proteins such as rituximab, required by regulatory authorities in the characterization of new biopharmaceuticals, could be successfully addressed as a practical use case of SEC-CERS. In addition, the quantification of functional excipients such as the disaccharide sucrose by SEC-CERS demonstrated the high applicability of the online coupled approach in the characterization of biopharmaceutical drug products.

Hemoglobin interferes with common analysis techniques applied for serum analysis which usually results in the disposal of hemolyzed samples,[1] underlining the complexity of the sample analyzed by SEC-CERS. Biomarkers such as serum albumin, immunoglobulin G and hemoglobin could be successfully identified in hemolyzed serum based on reference spectra and reliably differentiated from each other by a hit quality index (HQI). The investigation of different binding and oxidation states of the heme prosthetic group revealed that oxygen binding is not accessible with SEC-CERS as oxygenation reaches an equilibrium state under the conditions of SEC. Oxidation of the heme group was irreversible under the conditions of the SEC which resulted in the reliable detection of methemoglobin.

Identification based on visual inspection can be biased, therefore, HQI and principal component analysis (PCA) have been investigated to provide an objective measure of identification. HQI provided a more objective measure of the similarity of two distinct spectra than visual inspection. In comprehensive analysis of different biopharmaceutical products carried out with the monoclonal antibodies daratumumab, bevacizumab, and rituximab, HQI ≥ 0.95 could be achieved for spectra of the same antibody acquired in different runs. In serum, the highest HQI of 0.91 ± 0.01 could be

achieved for the protein class of serum albumins where bovine and porcine serum albumins were compared for HQI evaluation. However, for the other fractions lower HQI (ranging between 0.39 – 0.88) and particularly higher variances in the HQI between different runs of the same fraction were observed likely due to interferences caused by fluorescence such as differences in data processing and in the noise level. On the other hand, not matching spectra, i.e. spectra of different protein classes, resulted in a mean HQI of 0.07 ± 0.06. Thus, HQI allowed for a more comprehensible identification of various protein classes. In conclusion, the HQI is an appropriate tool to objectively measure the similarity between spectra which is necessary to reliably differentiate between spectra. However, the application of HQI is limited to direct comparison of two spectra and does not enable to potentially recognize regions which influence the HQI more significantly. PCA applied to SEC-CERS data of a chimeric, a humanized and a human IgG1 antibody in biopharmaceutical products indicated distinct, but subtle differences between the antibodies despite them all being the same class of antibodies (IgG1). In combination with the excipients, the three biopharmaceutical products could be distinguished unambiguously, which is in line with another study on the differentiation of IgG antibodies in formulation.[2] The results of the PCA demonstrated the applicability of SEC-CERS to differentiate biopharmaceutical products which could be of interest in the quality control of biopharmaceutical products to analyze batch-to-batch consistency of the higher-order structure. In combination with a diode-array detector (DAD), SEC-DAD-CERS could be effectively applied to simultaneously analyze the molecular size and higher-order structure of the protein, while performing an impurity analysis regarding aggregate formation and quantity. Thus, SEC-DAD-CERS could be an effective approach to shorten analysis time and reduce costs by combining different techniques. However, since the data set was limited in this thesis, additional experiments on different batches and IgG1 antibodies must be performed to elaborate the applicability of SEC-CERS for quality control of monoclonal antibodies.

The automated data processing and evaluation workflows applied for the comprehensive analysis of biopharmaceutical products and the data sets used in chapter 4 are available in a repository. This ensures the reproducibility of the workflows by other researchers and effectively shares data processing in science, besides contributing to the FAIR data principle.[3]

For many proteins, Raman spectra of high quality could be acquired meaning that in addition to a high signal-to-noise ratio also lower intense bands could be clearly observed. However, due to the inherently low sensitivity of the Raman effect, the concentration of protein must be sufficiently high to enable the acquisition of appropriate Raman spectra. The concentration of common biopharmaceutical concentrates for preparation of parenteral dosage forms was sufficiently high for SEC-CERS analysis. However, in serum only the high abundance proteins could be analyzed outlining a limitation of the online coupled system. Besides, the resolution of the SEC affected the sensitivity of the CERS detector and potentially led to co-elution of other compounds that could not be detected. Furthermore, aggregated species

could be observed for all proteins in chapter 2. However, it was not possible to retrieve Raman spectra of the aggregated species as demonstrated in Figure S2-2 in the supporting information of chapter 2. In particular, the structural analysis and recognition of aggregates is important in pharmaceutical quality control and in medicine. Aggregates potentially cause adverse immune response if administered to patients[4] and therefore, the detection of aggregate levels is an important parameter in pharmaceutical quality control. In medical context, the analysis of aggregates is of interest to detect neurodegenerative diseases such as Parkinson's or Alzheimer's disease which are caused by the misfolding and fibrillar aggregation of certain proteins.[5, 6] Thus, the analysis of aggregates would be an interesting field for investigation with SEC-CERS. However, the current set-up cannot detect soluble aggregates due to their relatively low concentration compared to the monomeric proteins. The sensitivity of SEC-CERS must be increased to investigate soluble aggregates which might be done by increasing the length of the liquid core waveguide (LCW). Therefore, future studies on CERS could focus on optimizing the length of the LCW.

Within the thesis, the length of the LCW was kept at 20 cm length with an inner volume of approximately 6.5 µL to enable comparable results between the different chapters. According to the literature[7-10] an increase in signal intensity for CERS might be possible by increasing the length of the LCW; especially considering the relatively broad peak widths of SEC that were observed in chapters 2 – 4. Thus, this might be an option to detect, e.g. aggregates, as mentioned before. However, band broadening and other chromatographic parameters such as different mobile phases, various inner diameters and the flow rate must be accounted for and therefore, the optimum length needs to be investigated in detail, which was beyond the scope of the thesis.

Furthermore, chapter 3 demonstrated resonance enhancement of the heme prosthetic group, which provided highly selective information on the binding and oxidation state of heme. Laser wavelengths in the deep UV range can resonantly excite certain vibrations of the peptide backbone or various amino acid side chains if the laser line coincides with an absorption band, which could be a promising opportunity to increase sensitivity of the CERS detector and to study changes in protein conformation, e.g. due to aggregation.[11] However, changing the laser wavelength from visible to deep UV, would require optimization / replacement of the optical components such as the spectrograph, CCD camera and edge filter, to match the deep UV range for detection of resonance Raman scattering. Therefore, this needs to be investigated in future studies.

An alternative to SEC might be the coupling of CERS with other separation techniques such as flow field-flow fractionation to increase insights into protein aggregation, since flow field-flow fractionation enables the separation of aggregates beyond the size limits of SEC.[12] In addition, an online coupling of CERS to other biochromatographic modes such as ion exchange chromatography (IEX) and hydrophobic interaction chromatography (HIC) could be investigated. Both techniques are based on gradient elution of aqueously buffered eluents which are compatible with CERS but will pose

an additional challenge to the data processing due to a changing background signal from the mobile phase caused by gradient elution. On the other hand, peak width will presumably decrease due to the gradient, leading to higher concentrations within the peak maximum, which could be advantageous to overcome the relatively low sensitivity of CERS detector. The high salt concentrations applied in HIC might alter the native structure of the proteins, but this needs to be investigated more in detail in future studies on the online coupling of CERS to liquid chromatography.

In addition, future studies could address other biopharmaceutical active ingredients such as antibody-drug conjugates or polypeptides. The combination of biochromatography and CERS detection can be used to investigate their three-dimensional structure and, in case of antibody-drug conjugates, may provide information on the amount of drug loading.

5.1 References

(1) D.K.R. Medipally; D. Cullen; V. Untereiner; J. Bryant; G.D. Sockalingum; T.N.Q. Nguyen; E. Noone; S. Bradshaw; M. Finn; M. Dunne; et al., Effect of hemolysis on Fourier transform infrared and Raman spectra of blood plasma. *J. Biophotonics* **2020**, *13* (7), e201960173. DOI: 10.1002/jbio.201960173.

(2) M.K. Shukla; P. Wilkes; N. Bargary; K. Meagher; D. Khamar; D. Bailey; S.P. Hudson, Identification of monoclonal antibody drug substances using non-destructive Raman spectroscopy. *Spectrochim. Acta, Part A* **2023**, *299*, 122872. DOI: 10.1016/j.saa.2023.122872.

(3) M.D. Wilkinson; M. Dumontier; I.J. Aalbersberg; G. Appleton; M. Axton; A. Baak; N. Blomberg; J.-W. Boiten; L.B. da Silva Santos; P.E. Bourne; et al., The fair guiding principles for scientific data management and stewardship. *Sci. Data* **2016**, *3* (1), 160018. DOI: 10.1038/sdata.2016.18.

(4) H.C. Mahler; W. Friess; U. Grauschopf; S. Kiese, Protein aggregation: Pathways, induction factors and analysis. *J. Pharm. Sci.* **2009**, *98* (9), 2909-2934. DOI: 10.1002/jps.21566.

(5) G. Devitt; K. Howard; A. Mudher; S. Mahajan, Raman spectroscopy: An emerging tool in neurodegenerative disease research and diagnosis. *ACS Chem. Neurosc.* **2018**, *9* (3), 404-420. DOI: 10.1021/acschemneuro.7b00413.

(6) G. Devitt; W. Rice; A. Crisford; I. Nandhakumar; A. Mudher; S. Mahajan, Conformational evolution of molecular signatures during amyloidogenic protein aggregation. *ACS Chem. Neurosc.* **2019**, *10* (11), 4593-4611. DOI: 10.1021/acschemneuro.9b00451.

(7) R. Altkorn; M. Duval Malinsky; R.P. van Duyne; I. Koev, Intensity considerations in liquid core optical fiber Raman spectroscopy. *Appl. Spectrosc.* **2001**, *55* (4), 373-381. DOI: 10.1366/0003702011951939.

(8) R. Altkorn; I. Koev; M.J. Pelletier, Raman performance characteristics of Teflon-AF 2400 liquid-core optical-fiber sample cells. *Appl. Spectrosc.* **1999**, *53* (10), 1169-1176. DOI: 10.1366/0003702991945560.

(9) R. Altkorn; I. Koev; R.P. Van Duyne; M. Litorja, Low-loss liquid-core optical fiber for low-refractive-index liquids: Fabrication, characterization, and application in Raman spectroscopy. *Appl. Opt.* **1997**, *36* (34), 8992-8998. DOI: 10.1364/AO.36.008992.

(10) R.J. Dijkstra; C.T. Martha; F. Ariese; U.A.T. Brinkman; C. Gooijer, On-line identification method in column liquid chromatography: UV resonance Raman spectroscopy. *Anal. Chem.* **2001**, *73*, 4977-4982. DOI: 10.1021/ac0103569.

(11) R.S. Jakubek; J. Handen; S.E. White; S.A. Asher; I.K. Lednev, Ultraviolet resonance Raman spectroscopic markers for protein structure and dynamics. *TrAC, Trends Anal. Chem.* **2018**, *103*, 223-229. DOI: 10.1016/j.trac.2017.12.002.

(12) D.C. Rambaldi; P. Reschiglian; A. Zattoni, Flow field-flow fractionation: Recent trends in protein analysis. *Anal. Bioanal. Chem.* **2011**, *399* (4), 1439-1447. DOI: 10.1007/s00216-010-4312-5.

6 Summary

Coupling of liquid chromatography (LC) with various spectroscopic methods such as UV/Vis spectroscopy has been common practice since the 1980s. However, to date, relatively few studies have investigated the online coupling of LC with Raman spectroscopy (RS). In particular, RS provides selective information on the conformation and structural elements of proteins, enabling non-destructive and label-free analysis of proteins under native conditions. In recent studies, mainly pure substances or mixtures of selected analytes were analyzed by RS detection after chromatographic separation, rather than compounds in a complex matrix.

Therefore, the focus of this work was to examine the possibilities and limitations of online coupling LC with RS for analyzing proteins and their prosthetic groups in biopharmaceutical or biological samples, thereby addressing various bioanalytical questions. Size exclusion chromatography (SEC) was chosen as separation technique for coupling due to its relevance in the characterization of biopharmaceuticals. The aqueous buffer solutions used for SEC elution provide native conditions for proteins and are highly compatible with RS detection. Within the scope of this work, proteins in biopharmaceutical drugs and hemolyzed serum were examined, identified, and differentiated based on their structure. In addition, automated data evaluation and assessment of spectral differences and similarities, as well as the quantification of functional excipients in a biopharmaceutical formulation were investigated. The setup of the coupled system was described in detail, and the term capillary-enhanced Raman spectroscopy (CERS) was coined for the detection system.

The online coupling SEC-CERS was successfully applied to the structural elucidation, identification, and differentiation of various proteins in different samples, such as biopharmaceuticals and blood serum. SEC-CERS was suitable for the simultaneous determination of the conformation of therapeutic proteins and the quantification of functional excipients in biopharmaceuticals, which can contribute to the comprehensive characterization of biopharmaceuticals required by regulatory authorities. Furthermore, the biomarkers serum albumin, immunoglobulin G, and hemoglobin were successfully identified in hemolyzed serum. However, a limitation is that protein concentration must be sufficiently high for analysis. Thus, while biopharmaceutical formulations could be analyzed, only high abundance proteins were accessible in serum. Automated data evaluation and principal component analysis enabled differentiation of three IgG1 antibodies as individual active substances as well as in their formulations, thereby demonstrating another potential application in pharmaceutical quality control by detecting differences between protein samples or identifying similarities.

In summary, this thesis addresses several practical application examples in the field of protein analysis using SEC-CERS, which demonstrates a significant research contribution in the field of RS detection for LC.

7 Zusammenfassung

Die Kopplung der Flüssigkeitschromatographie (LC) mit unterschiedlichen spektroskopischen Methoden wie beispielsweise der UV/Vis-Spektroskopie ist seit den 1980er Jahren gängige Praxis. Jedoch gibt es bis heute nur relativ wenige Studien zu einer Online-Kopplung aus LC und Raman Spektroskopie (RS). Dabei ermöglicht die RS insbesondere im Bereich der Proteinanalytik selektive Informationen zur Konformation und zu den Strukturelementen von Proteinen, die unter nativen Bedingungen zerstörungs- und markierungsfrei analysiert werden können. Im Rahmen von bisherigen Studien wurden hauptsächlich reine Substanzen oder Mischungen daraus mittels RS-Detektion nach chromatographischer Trennung analysiert, jedoch kaum reale Proben. Der Fokus dieser Arbeit lag daher auf der Erforschung der Möglichkeiten und Grenzen einer Online-Kopplung aus LC und RS zur Untersuchung von Proteinen und ihren prosthetischen Gruppen in biopharmazeutischen oder biologischen Proben, wobei verschiedene bioanalytische Fragestellungen adressiert werden sollten. Die Größenausschlusschromatographie (SEC) wurde aufgrund ihrer Relevanz in der Charakterisierung von Biopharmazeutika als Trenntechnik zur Kopplung ausgewählt. Die wässrigen Pufferlösungen zur Elution der SEC bieten native Bedingungen für Proteine und sind kompatibel mit der RS-Detektion. Im Rahmen der durchgeführten Arbeiten wurden Proteine in biopharmazeutischen Arzneimitteln und hämolysiertem Serum hinsichtlich ihrer Struktur untersucht, identifiziert und differenziert. Zusätzlich wurden die Aspekte der automatisierten Datenauswertung und Bewertung von spektralen Unterschieden bzw. Übereinstimmungen sowie die Quantifizierung von funktionalen Hilfsstoffen in einem Biopharmazeutikum im Rahmen der Arbeit untersucht. Der Aufbau des gekoppelten Systems wurde detailliert beschrieben und dabei der Ausdruck „kapillar-verstärkte Raman Spektroskopie (CERS)“ für das Detektionssystem geprägt. Die Online-Kopplung SEC-CERS konnte erfolgreich zur Strukturaufklärung, Identifizierung und Unterscheidung verschiedener Proteine in unterschiedlichen Proben wie Biopharmazeutika oder Blutserum eingesetzt werden. SEC-CERS eignete sich zur simultanen Bestimmung der Konformation von therapeutischen Proteinen und zur Quantifizierung von funktionalen Hilfsstoffen in Biopharmazeutika, was zur umfangreichen Charakterisierung von Biopharmazeutika seitens der regulatorischen Behörden beitragen kann. Zusätzlich konnten die Biomarker Serumalbumin, Immunglobulin G und Hämoglobin erfolgreich in hämolysiertem Serum identifiziert werden. Jedoch zeigte sich, dass die Konzentration der analysierten Proteine ausreichend hoch sein muss. Somit konnten biopharmazeutische Arzneiformen analysiert werden, während in Serum nur die in höherer Konzentration auftretenden Proteine zugänglich waren. Drei IgG1 Antikörper konnten als einzelne Wirkstoffe sowie unter Berücksichtigung der Formulierung durch automatisierte Datenauswertung und den Einsatz einer Hauptkomponentenanalyse voneinander unterschieden werden, wodurch ein weiteres potenzielles Anwendungsfeld in der pharmazeutischen Qualitätskontrolle mit der Erkennung von Unterschieden bzw. der Identifizierung von Ähnlichkeiten zwischen Proteinproben adressiert werden konnte. Zusammenfassend konnten im Rahmen dieser Arbeit verschiedene praktische Anwendungsbeispiele aus dem Bereich der Proteinanalytik mit SEC-CERS adressiert werden, was einen wesentlichen Beitrag zur Forschung im Bereich der RS-Detektion für die LC darstellt.

8 List of Publications

8.1 Included in this thesis

Jana Thissen, Martin D. Klassen, Björn Fischer, Michael C. Hacker, Jörg Breitkreutz, Thorsten Teutenberg & Ricardo Cunha
StreamFind: data processing workflows for qualification and quantification of biopharmaceutical drug products analyzed by size exclusion chromatography coupled to capillary-enhanced Raman spectroscopy
Anal. Bioanal. Chem. **2025**, *417* (19), 4469 – 4480, DOI: 10.1007/s00216-025-05964-3.

Jana Thissen, Martin D. Klassen, Michael C. Hacker, Jörg Breitkreutz, Thorsten Teutenberg & Björn Fischer
Online coupling of size exclusion chromatography to capillary-enhanced Raman spectroscopy for the identification of protein classes in hemolyzed blood serum
Anal. Bioanal. Chem. **2025**, *417* (2), 335 – 344, DOI: 10.1007/s00216-024-05649-3.

Jana Thissen, Martin D. Klassen, Philipp Constantinidis, Michael C. Hacker, Jörg Breitkreutz, Thorsten Teutenberg & Björn Fischer
Online coupling of size exclusion chromatography to capillary enhanced Raman spectroscopy for the analysis of proteins and biopharmaceutical drug products
Anal. Chem. **2023**, *95* (48), 17868 – 17877, DOI: 10.1021/acs.analchem.3c03991.

8.2 Other publications

Jana Thissen, Lars M. H. Reinders, Jochen Tuerk & Martin D. Klassen
Cleaning validation of different cleaning procedures for monoclonal antibodies on stainless steel
European Journal of Oncology Pharmacy, **2026**, 9:1 (e60), DOI: 10.1097/OP9.0000000000000060.

Kjell Kochale, Jana Thissen, Ricardo Cunha, Stefan Lamotte, Thorsten Teutenberg & Torsten C. Schmidt,
Enrichment and quantification of 18 polycyclic aromatic hydrocarbons from intermediates for plastics production by a generic liquid chromatography column switching
J. Sep. Sci. **2023**, *46* (14), DOI: 10.1002/jssc.202300076.

9 List of Contributions

9.1 Oral presentations

Jana Thissen, Martin D. Klassen, Michael C. Hacker, Jörg Breitkreutz, Thorsten Teutenberg & Björn Fischer
Potential of Raman spectroscopic detection coupled to size exclusion chromatography for the analysis of therapeutic proteins and disaccharides
35. Doktorandenseminar des Arbeitskreises Separation Science der Gesellschaft Deutscher Chemiker e. V., Hohenroda, Germany
12.01.2025 – 14.01.2025

Jana Thissen, Martin D. Klassen, J. Ricardo Cunha, Philip Wenig, Michael C. Hacker, Jörg Breitkreutz, Thorsten Teutenberg & Björn Fischer
Online coupling of size exclusion chromatography to Raman spectroscopy for the analysis of therapeutic proteins and disaccharides
18th International Symposium on Hyphenated Techniques in Chromatography and Separation Technology (HTC-18), Leuven, Belgium
28.05.2024 - 31.05.2024

Jana Thissen, Martin D. Klaßen, Michael C. Hacker, Jörg Breitkreutz, Thorsten Teutenberg & Björn Fischer
Online coupling of size exclusion chromatography to Raman spectroscopy for protein analysis
5th Braunschweig International Symposium on Pharmaceutical Engineering Research (SPhERe 2023), Braunschweig, Germany
18.10.2023 – 20.10.2023

Jana Thissen, Martin D. Klassen, Michael C. Hacker, Jörg Breitkreutz, Thorsten Teutenberg & Björn Fischer
Online coupling of size exclusion chromatography to Raman spectroscopy for protein analysis
ANAKON 2023, Vienna, Austria
11.04.2023 – 14.04.2023

Jana Thissen, Martin D. Klassen, Thorsten Teutenberg, Björn Fischer, Michael C. Hacker & Jörg Breitkreutz
Application and validation of online coupled size exclusion chromatography to capillary enhanced Raman spectroscopy (SEC-CERS)
Moderne Trenn- und Detektionsmethoden für Antikörper und Proteine – BioLC Seminar 2022, Online, YMC Europe GmbH
27.09.2022

9.2 Poster presentations

Jana Thissen, Martin D. Klassen, Björn Fischer, Thorsten Teutenberg & J. Ricardo Cunha
StreamFind: Facilitating identification, quantitation and qualification of different biopharmaceutical products analyzed by applying size exclusion chromatography coupled to capillary-enhanced Raman spectroscopy
ANAKON 2025, Leipzig, Germany
10.03.3025 – 13.03.2025

J. Ricardo Cunha, Jana Thissen, Walter Laurito, Steffen Thoma, Martin D. Klassen & Thorsten Teutenberg
StreamFind: Data processing workflow designer for non-target screening and highly hyphenated analytical systems
18th International Symposium on Hyphenated Techniques in Chromatography and Separation Technology (HTC-18), Leuven, Belgium
28.05.2024 - 31.05.2024

Jana Thissen, Martin D. Klaßen, J. Ricardo Cunha, Philip Wenig, Michael C. Hacker, Jörg Breitkreutz, Thorsten Teutenberg & Björn Fischer
Automated data processing of Raman spectra from online coupled size exclusion chromatography to Raman spectroscopy for protein analysis
HPLC 2023, Düsseldorf, Germany
18.06.2023 – 22.06.2023

Jana Thissen, Martin D. Klassen, Philipp Constantinidis, Michael C. Hacker, Jörg Breitkreutz, Thorsten Teutenberg & Björn Fischer
Technical development for the hyphenation of size exclusion chromatography to Raman spectroscopy
ANAKON 2023, Vienna, Austria
11.04.2023 – 14.04.2023
Invitation to the poster pitch finals of the 25 best posters.

9.3 Other contributions

Martin Klaßen, Jana Thissen, Thorsten Teutenberg
Online-Ramandetektion in der Serumanalytik - Kopplung von Chromatographie und Ramanspektroskopie
GIT Labor-Fachzeitschrift, John Wiley & Sons, Hoboken, NJ, USA
07.04.2025
URL: https://analyticalscience.wiley.com/content/article-do/online-ramandetektion-der-serumanalytik

John Chasse
Interview on: Coupling Size Exclusion Chromatography and Capillary-Enhanced Raman Spectroscopy for Analysis of Hemolyzed Serum Samples
LCGC International & Spectroscopy Online, MJH Life Sciences, Cranbury, NJ, USA
17.02.2025
LCGC International: https://www.chromatographyonline.com/view/coupling-size-exclusion-chromatography-and-capillary-enhanced-raman-spectroscopy-for-analysis-of-hemolyzed-serum-samples
Spectroscopy Online: https://www.spectroscopyonline.com/view/coupling-size-exclusion-chromatography-and-capillary-enhanced-raman-spectroscopy-for-analysis-of-hemolyzed-serum-samples

J. Ricardo Cunha, Jana Thissen, Walter Laurito, Steffen Thoma, Martin D. Klassen & Thorsten Teutenberg
StreamFind: Software-Tool zur Datenverarbeitung – Flexibler Workflow-Designer für verschiedene Anwendungen
GIT Labor-Fachzeitschrift, John Wiley & Sons, Hoboken, NJ, USA
02.05.2024
URL: https://analyticalscience.wiley.com/content/article-do/streamfind-software-tool-zur-datenverarbeitung

Jana Thissen, Martin D. Klaßen & Thorsten Teutenberg
Moderne biochromatographische Verfahren und Detektionssysteme zur Analytik von therapeutischen Proteinen - Aktuelle Forschungsthemen in der Bioanalytik
GIT Labor-Fachzeitschrift, John Wiley & Sons, Hoboken, NJ, USA
10.04.2024
URL: https://analyticalscience.wiley.com/content/article-do/moderne-biochromatographische-verfahren-und-detektionssysteme-zur-analytik-von

10 Danksagung

Zuerst möchte ich mich bei meinem Doktorvater Prof. Dr. Jörg Breitkreutz für die Betreuung während meiner Promotion als externe Promovierende bedanken. Ich bedanke mich bei Ihnen für Ihre fachliche Unterstützung und Ihr entgegengebrachtes Vertrauen in meine Arbeit, wodurch ich mein Promotionsthema eigenständig gestalten konnte.

Bei meinem Mentor Jun.-Prof. Dr. Michael Hacker möchte ich mich für die freundliche Übernahme des Korreferats bedanken. Ich danke Ihnen darüber hinaus für die fachliche Unterstützung insbesondere bei den wissenschaftlichen Veröffentlichungen und für das entgegengebrachte Vertrauen bei der Gestaltung der Promotionsarbeit.

Mein besonderer Dank gilt Dr. Björn Fischer, Martin Klaßen und Dr. Thorsten Teutenberg für die intensive Betreuung, die Gesprächs- und Hilfsbereitschaft jederzeit, das Korrekturlesen und konstruktive Feedback zu diversen Abstracts, Postern, Publikationen, Vorträgen und der Dissertation. Zusätzlich bedanke ich mich bei dir, Björn, für deine beratende und tatkräftige Unterstützung bei Justagearbeiten und Reparaturen rund um das Raman-System, sowie für die von dir besorgten Ersatzteile für die Detektionszelle. Vielen Dank an Martin für deine tatkräftige Unterstützung bei Reparaturen jeglicher Art an der Detektionszelle oder der HPLC, das Besorgen von biologischen Proben, sowie den regelmäßigen, intensiven Austausch zu meinen Promotionsarbeiten. Zusätzlich danke ich dir, Thorsten, dass du mir die Teilnahme an mehreren verschiedenen wissenschaftlichen Tagungen und Konferenzen ermöglicht hast.

Zusätzlich möchte ich mich bei meinen Arbeitskolleginnen und -kollegen, insbesondere bei *denen da oben*, für die angenehme Arbeitsatmosphäre und Hilfsbereitschaft während meiner Promotion bedanken. Ein besonderer Dank gilt meinen Mitdoktorandinnen und Mitdoktoranden, Dr. Kjell Kochale, Dr. Tobias Werres, Dr. Lars Reinders und Dr. Michelle Klein, die mir während der gesamten Promotionszeit immer wieder mit Rat, Motivation und Unterstützung zur Seite standen. Darüber hinaus gilt mein besonderer Dank Dr. Ricardo Cunha für die gute Zusammenarbeit und Unterstützung bei der automatisierten Auswertung der Messdaten, die maßgeblich zum Gelingen der 3. Veröffentlichung beigetragen haben. Zusätzlich möchte ich mich bei dir, Kjell, für die tatkräftige Unterstützung bei der Umsetzung der elektronischen Signalweiterleitung zwischen der Agilent HPLC und dem Raman Detektor bedanken.

Mein herzlichster Dank gilt meinen Eltern Anna-Maria und Wilfried Thissen sowie meinem Bruder Martin Thissen für die stetige Unterstützung auf dem Weg zur Promotion und auf meinem gesamten Weg bis hierhin! Mein größter Dank gilt meinem Ehemann Sunny Thissen. Ich danke dir von Herzen für deine grenzenlose Unterstützung, deinen stetigen Zuspruch, deine Geduld und dein Verständnis während der gesamten Zeit. Ich danke euch allen von Herzen, denn ohne euch würde ich heute nicht hier stehen!

11 Eidesstattliche Erklärung

Ich versichere an Eides Statt, dass die Dissertation von mir selbständig und ohne unzulässige fremde Hilfe unter Beachtung der „Grundsätze zur Sicherung guter wissenschaftlicher Praxis an der Heinrich-Heine-Universität Düsseldorf“ erstellt worden ist. Die Dissertation wurde in der vorgelegten oder in ähnlicher Form noch bei keiner anderen Institution eingereicht. Ich habe bisher keinen erfolglosen Promotionsversuch unternommen.

_____

Jana Thißen